

Charles University in Prague, Czech Republic

1st Faculty of Medicine

Doctoral Study of Biomedicine

Human Physiology and Patophysiology

**MOLECULAR AND BIOCHEMICAL FEATURES OF THREE ENZYMES
THAT MAY SERVE AS NEW DRUG TARGETS IN *Cryptosporidium parvum***

A Dissertation by

Mgr. VLASTA ČTRNÁCTÁ

2008

Mentor: Doc. MUDR. MARIE STAŇKOVÁ, CSc.

ABSTRACT

Molecular and biochemical features of three enzymes that may serve as new drug targets in *Cryptosporidium parvum*.

(2008)

Mgr. Vlasta Čtrnáctá

Cryptosporidium parvum is a unicellular parasite belonging to the Phylum Apicomplexa. This parasite can infect both humans and animals, causing an acute diarrhea in immunocompetent persons, and a chronic life threatening infection in immunocompromised individuals. Although many drugs, to combat this parasite, have been empirically tested, there is no completely effective therapy to treat cryptosporidiosis in humans or animals. In recent years, the completion of the genome sequencing projects along with advances in molecular methods have significantly helped to increase our general understanding of the *C. parvum* metabolic machinery. However, our knowledge concerning many specific pathways and enzymes in *Cryptosporidium* is still limited. Their better understanding in this organism would aid in experimentation of new drugs and new strategy development to treat cryptosporidiosis in humans and animals.

The long-term research goal of our laboratory is to characterize the molecular and biochemical features of enzymes involved in the core metabolism of *C. parvum* in an effort to develop novel therapeutics. The specific objectives of our research described in this dissertation are:

1. To determine the subcellular localization of one of the core metabolic enzymes, pyruvate:NADP⁺ oxidoreductase (PNO), which is responsible for converting pyruvate to acetyl-CoA. This unique PNO is a fusion of an N-terminal pyruvate:ferredoxin oxidoreductase domain and a C-terminal cytochrome P-450 reductase domain. This protein has been found to target the mitochondria in the distantly related protist *Euglena gracilis*. The

determination of PNO localization either in the cytosol or in the relict mitochondrion of *C. parvum* is critical in assigning the enzyme biological role in this parasite.

2. To characterize a *Narf*-like gene in *Cryptosporidium* that resembles [Fe]-hydrogenases in other anaerobic protists and to explore this unique gene as a potential drug target.
3. To characterize S-adenosylhomocysteine hydrolase from *C. parvum*. This is an enzyme regulating the S-adenosylhomocysteine metabolic pathway, which has been considered important in the target-based drug design of antiviral and antiparasitic drugs. Therefore, recombinant enzyme can be used to evaluate the efficiency of potential inhibitors, leading to studies in elucidating their effect on the *in vitro* growth of *C. parvum*.

DEDICATION

This dissertation is dedicated to my beloved parents, Eliška and Josef Čtrnáctých, who always provide me with enormous support. I also appreciate that my father has kept asking me when will I finally finish my postgraduate program.

ACKNOWLEDGEMENTS

As the author of this dissertation, I would like to express my immense gratitude and sincere thanks to my mentor Doc. MUDR. Marie Staňková CSc., from the 3rd Department of Infectious and Tropical Diseases of the First Faculty of Medicine and Hospital Na Bulovce, Charles University in Prague, my supervisor RNDr. MUDR. František Stejskal, Ph.D. from the Department of Tropical Diseases of the 1st Faculty of Medicine, Charles University in Prague, RNDr. Ivan Hrdý, Ph.D. from the Department of Parasitology, the Faculty of Science, Charles University in Prague and our collaborators in the United States of America (USA), Professor Janet S. Keithly, Ph.D. from the Wadsworth Center, New York State Department of Health (NYS DOH), and Associate Professor Guan Zhu, Ph.D. from the Department of Veterinary Pathobiology, Texas A&M University for their guidance and support throughout the course of this research.

Thanks also go to my friends and colleagues, especially Jason M. Fritzler at Texas A&M University.

I also want to extend my gratitude to the Fogarty International Fellowship Program funded through the Fogarty International Center at the National Institutes of Health (NIH), which financially supported the research at the Wadsworth Center and Texas A&M University in the USA.

Finally, I would like to convey my appreciation to Prof. RNDr. Antonín Holý, D.Sc., Dr.h.c. from Institute of Organic Chemistry and Biochemistry in Prague, who has kindly provided several compounds that are indispensable to the research described in the dissertation.

ABBREVIATIONS

ACBP	Acyl-CoA Binding Protein
ACCase	Acetyl-CoA Carboxylase
ACS	Acyl-CoA Synthase
AdhE	Alcohol/Acetaldehyde Dehydrogenase, Type E
AdoMet	S-Adenosylmethionine
ADP	Adenosine Diphosphate
AIDS	Acquired Immunodeficiency Syndrome
AMP	Adenosine Monophosphate
Ara-A	9- β -D-Arabinofuranosyladenine
ATP	Adenosine Triphosphate
BLAST	Basic Local Alignment and Search Tool
BSA	Bovine Serum Albumin
CB	Crystalloid Body
CDC	Centers for Disease Control and Prevention
CoA	Coenzyme A
CPR	NADPH-Cytochrome P450 Reductase Domain
CTP	Cytidine Triphosphate
DAPI	4',6'-Diamidino-2-Phenyl Indole
DATP	Deoxyadenosine Monophosphate
DCTP	Deoxycytidine Triphosphate
DMSO	Dimethyl Sulfoxide
DNA	Deoxyribonucleic Acid
DNTB	5,5'-Dithiobis (2-Nitrobenzoic) Acid
EDTA	Ethylenediaminetetraacetic Acid
ELISA	Enzyme-Linked ImmunoSorbent Assay
EritA	D-Eritadenine (4-(9-Adenyl)-D-erythro-2,3-dihydroxybutyric acid)
FAD	Flavin Adenine Dinucleotide
FAS	Fatty Acid Synthase

FDA	Food and Drug Administration
FMN	Flavin Mononucleotide
gDNA	Genomic DNA
GMP	Guanosine Monophosphate
GTP	Guanosine Triphosphate
GSS	Genome-Sequencing Survey Project
HAART	Highly Active Anti-Retroviral Treatment
HBSS	Hanks' Balanced Salt Solution
HIV	Human Immunodeficiency Virus
HSP70	70-kDa Heat Shock Protein
IC ₅₀	50% Inhibitory Concentration
Ig	Immunoglobulin
IL	Interleukin
IMP	Inosine Monophosphate
INF	Interferon
IPTG	Isopropyl-1-Thio- β -D-galactopyranoside
LB	Luria-Bertani
LCE	Long Chain Elongase
LCFA	Long Chain Fatty Acid
LDH	Lactate Dehydrogenase
LGT	Lateral Gene Transfer
MBP	Maltose Binding Protein
MCMC	Markov Chain Monte Carlo
ML	Maximal Likelihood
MTT	Cell Viability Assay
Mr	Molecular Weight
NAD(H)	Nicotinamide Adenine Dinucleotide
NADP(H)	Nicotinamide Adenine Dinucleotide Phosphate
NARF	Nuclear Prelamin A Recognition Factor
NTZ	Nitazoxanide
PAGE	Polyacrylamide Gel Electrophoresis
PBS	Phosphate Buffered Saline

PCR	Polymerase Chain Reaction
PDB	Protein Database
PDH	Pyruvate Dehydrogenase Complex
PPi-PFK	Pyrophosphate-Dependent Phosphofructokinase
PFL	Pyruvate Formate Lyase
PFO	Pyruvate:Ferredoxin Oxidoreductase
PKS	Polyketide Synthase
PNO	Pyruvate:NADP ⁺ Oxidoreductase
pMAL	The vector that is designed to produce maltose-binding protein fusion
PPi	Inorganic Pyrophosphate
PPTase	Cytosolic Fatty Acid Phosphopantetheinyl Transferase
PRM	Paromomycin
qRT-PCR	Quantitative Reverse Transcriptase Polymerase Chain Reaction
(R)-DHAP	(R)-9-(2,3-Dihydroxypropyl)Adenine
RNA	Ribonucleic Acid
rRNA	Ribosomal Ribonucleic Acid
SAHH	S-Adenosylhomocysteine Hydrolase
SAMS	S-Adenosyl-L-Methionine Synthase
(S)-DHAP	(S)-9-(2,3-Dihydroxypropyl)Adenine
SDS	Sodium Dodecyl Sulfate
SSU rRNA	Small Subunit Ribosomal Ribonucleic Acid
TEM	Transmission Electron Microscopy
TNB	5-Thio-2-Nitrobenzoate
TTP	Thymidine Triphosphate
UTP	Uridine Triphosphate
XMP	Xanthosine Monophosphate

TABLE OF CONTENTS

		Page
ABSTRACT		iii
DEDICATION		v
ACKNOWLEDGEMENTS		vi
ABBREVIATIONS.....		vii
TABLE OF CONTENTS		x
LIST OF FIGURES.....		xiii
LIST OF TABLES		xv
GENERAL INTRODUCTION TO <i>Cryptosporidium</i>		
I	HISTORY.....	1
II	PHYLOGENY AND TAXONOMY	2
III	ULTRASTRUCTURE	3
IV	THE LIFE CYCLE.....	5
V	CRYPTOSPORIDIOSIS	8
	Outbreaks and routes of transmission of cryptosporidiosis	8
	Global distribution of cryptosporidiosis.....	9
	Human cryptosporidiosis in the Czech Republic	11
VI	OOCYSTS AND WATER TREATMENT.....	12
	Oocysts and their resistance to common infectants.....	12
	Infectivity	13
	Water treatment	13
VII	HUMAN DISEASE	15
	Clinical manifestation	15
	Pathogenesis and immunology of the disease	15
	Diagnosis	17
	Therapy.....	17
VIII	GENOME.....	19
IX	BIOCHEMICAL PROCESSES	20
	The fate of glucose	20

	The fate of pyruvate	22
	Fatty acid synthesis	23
	Nucleic acid synthesis	24
	Amino acid synthesis	25
	Methionine cycle and polyamine synthesis.....	25
	AIMS OF THE DISSERTATION	27
	METHODS	
I	ORGANISMS	28
	<i>Euglena gracilis</i> - culturing.....	28
	<i>Cryptosporidium parvum</i>	28
	The human colorectal cell line HCT-8 – culturing and parasite infection.....	29
	<i>Escherichia coli</i> – culturing	29
II	NUCLEIC ACID METHODS	30
	Library screening, subcloning, sequencing	30
	Alignments and phylogenetic analysis	30
	DNA and RNA isolation	31
	Southern blot	31
	RT-PCR analysis for gene expression.....	31
	qRT-PCR.....	32
III	PROTEIN METHODS.....	32
	Cloning and expression of <i>pMAL-CpSAHH</i>	32
	Purification of <i>pMAL-CpSAHH</i>	33
	Cleavage of <i>MBP-CpSAHH</i> with Factor Xa	33
	Purification of <i>CpSAHH</i> on hydroxyapatite column and determination of its size	33
	SAHH activity assay	34
	SAHH inhibition assay.....	34
	Western blot	35
	Peptide competition assay for specificity of antibodies.....	35
IV	MICROSCOPY: LOCALIZATION	35
	Confocal microscopy.....	36
	Transmission electron microscopy.....	36
	RESULTS AND DISCUSSIONS	
I	LOCALIZATION OF PYRUVATE:NADP ⁺ OXIDOREDUCTASE (PNO) IN SPOROZOITES OF <i>Cryptosporidium parvum</i>	
	PNO in <i>Euglena gracilis</i> mitochondrion.....	38

	PNO in <i>Cryptosporidium parvum</i>	39
	PNO, its fragments and evolution	39
	Results	41
II	A <i>Narf</i> -LIKE GENE FROM <i>Cryptosporidium parvum</i> RESEMBLES HOMOLOGUES OBSERVED IN ANAEROBIC PROTISTS AND HIGHER EUKARYOTES	
	[Fe]-hydrogenases in hydrogenosomes	47
	[Fe] hydrogenases versus NARF-like proteins	48
	Results	49
III	CHARACTERIZATION OF S-ADENOSYLHOMOCYSTEINE HYDROLASE FROM <i>Cryptosporidium parvum</i>	
	S-adenosylmethionine metabolic pathway	54
	SAHH from different organisms	55
	Results	56
	Unpublished results	61
	SUMMARY	
	Pyruvate:NADP ⁺ oxidoreductase	66
	S-adenosylhomocysteine hydrolase	67
	<i>CpNARF</i> gene.....	68
	REFERENCES	69
	APPENDIX A: Article 1 – Localization of Pyruvate:NADP ⁺ Oxidoreductase in Sporozoites of <i>Cryptosporidium parvum</i>	87
	APPENDIX B: Article 2 – A <i>Narf</i> -Like Gene from <i>Cryptosporidium parvum</i> Resembles Homologues Observed in Anaerobic Protists and Higher Eukaryotes ...	95
	APPENDIX C: Article 3 – Characterization of S-Adenosylhomocysteine Hydrolase from <i>Cryptosporidium parvum</i>	102
	CURRICULUM VITAE	112

LIST OF FIGURES

	Page
Figure 1	Transmission electron microscopy of <i>Cryptosporidium parvum</i> sporozoite 5
Figure 2	The life cycle of <i>Cryptosporidium</i> 8
Figure 3	The module organization of <i>C. parvum</i> PFO/CPR gene and its prokaryotic and eukaryotic homologues. 40
Figure 4	Western blot analyses of sonicated extracts from <i>Cryptosporidium parvum</i> and <i>Euglena gracilis</i> , respectively 42
Figure 5 - 8	Confocal microscopic immunolocalization of pruvate:NADP ⁺ oxidoreductase in <i>Cryptosporidium parvum</i> sporozoites..... 44
Figure 9 - 10	The uptake of MitoTrackerGreen FM into the mitochondrion and crystalloid body of <i>Cryptosporidium parvum</i> sporozoites 45
Figure 11 - 14	Transmission electron microscopy of <i>Cryptosporidium parvum</i> sporozoites showing immunogold localization of pruvate:NADP ⁺ oxidoreductase..... 46
Figure 15	Prokaryotic and eukaryotic hydrogenase homologues..... 48
Figure 16	Southern blot and RT-PCR analysis of CpNARF..... 50
Figure 17	Multiple sequence alignment of conserved residues of [Fe]-hydrogenase homologues 51
Figure 18	Phylogenetic relationship among major [Fe]-hydrogenase clusters . 52
Figure 19	S-adenosylmethionine metabolic pathway..... 55
Figure 20	Partial alignment of CpSAHH and 12 other organisms 57
Figure 21	RT-PCR analysis of CpSAHH expression in <i>Cryptosporidium parvum</i> sporozoites..... 58
Figure 22	SDS-PAGE analysis of the purification of the recombinant SAHH. 58
Figure 23	Michaelis–Menten kinetics of MBP-CpSAHH and CpSAHH 59
Figure 24	Efficacy of (S)-DHPA on the growth of <i>C. parvum in vitro</i> , as determined by qRT-PCR..... 62
Figure 25	Efficacy of (R)-DHPA on the growth of <i>C. parvum in vitro</i> , as

	determined by qRT-PCR.....	62
Figure 26	Efficacy of EritA on the growth of <i>C. parvum in vitro</i> , as determined by qRT-PCR.....	63

LIST OF TABLES

	Page
Table 1	Incidence of cryptosporidiosis among patients in the Czech Republic 11
Table 2	Comparison of <i>Cryptosporidium parvum</i> SAHH activity with SAHH activities from other organisms measured in the hydrolytic direction. 60
Table 3	Effect of nucleoside analogues on the activity of recombinant CpSAHH 61

GENERAL INTRODUCTION TO *Cryptosporidium*

I HISTORY

Approximately 100 years ago (1907), Ernest Edward Tyzzer described an unknown protozoan in the gastric mucosa of asymptomatic mice, which he later named *Cryptosporidium muris* (Tyzzer, 1907). In 1912, he published a study that described *C. parvum* isolated from small intestine of mice (Tyzzer, 1912). *C. parvum* is one of the most troublesome species of *Cryptosporidium*, causing diarrheal illnesses in both humans and animals. The initial discovery of *C. parvum* did not attract much attention, partly because *Cryptosporidium* was not regarded as a pathogen until 1955 when it was associated with an outbreak of diarrhea in a turkey flock (Slavin, 1955). The first case of cryptosporidiosis in humans was observed 21 years later in a 3-year old child with enterocolitis (Nime *et al.*, 1976), in spite of this, cryptosporidiosis was still not regarded as a threat to humans. This changed during 1980s when *Cryptosporidium* infection was found to have caused the first deaths of patients with acquired immunodeficiency syndrome (AIDS) (Pitlik *et al.*, 1983). Cryptosporidiosis, practically unknown before the AIDS outbreak, has become one of the most common intestinal protozoan infections in both immunocompromised and immunocompetent persons. Since then, research on *Cryptosporidium* has expanded, and a wide range of new molecular features has been discovered through conventional experimental studies. These include identification of new organelles, metabolic pathways, therapeutic targets and characterization of inhibitors. Even more importantly, both the *C. parvum* and *C. hominis* genomes have been sequenced (Xu *et al.*, 2004; Abrahamsen *et al.*, 2004) revealing all nuclear-encoded sequences. These genome analyses confirmed the reduction and streamlining of metabolic pathways in *Cryptosporidium* and further clarified potential parasite-specific drug targets. Despite these numerous advances there is still no reliable vaccine or drug available for treating humans infected with cryptosporidiosis.

II PHYLOGENY AND TAXONOMY

With the aid of electron microscopy many unique features of *Cryptosporidium* were identified that confirmed the taxonomic position of this parasite into the Phylum Apicomplexa. This phylum contains many medically important pathogens, all intracellular, and it is divided into four major classes: Gregarina (gregarines, *Monocystis*); Coccidia (*Eimeria*, *Toxoplasma*, *Cyclospora*); Haemosporida (*Plasmodium*); and Piroplasmida (*Theileria*, *Babesia*). The most fundamental difference among these classes is the number of gametes produced during gamogony. *Cryptosporidium* has a single macro- and microgamete which fuse to form a zygote that becomes an oocyst. Therefore, this genus was placed within the Class Coccidia. However, there are unique features that clearly distinguish *Cryptosporidium* from Coccidia and other apicomplexan protozoa: i) the unusual localization of within the host cell (i.e. sequestered between the host cell cytoplasm and the cell membrane); ii) the absence of flagellated microgametes; iii) the secondary loss of the plastid; iv) the presence of a highly reduced mitochondrion; v) the autoinfection that occurs within the host; vi) an apparent innate resistance to antimicrobials; and vii) general absence of host specificity (especially *C. parvum*). These structural details together with recent molecular and phylogenetic studies are congruent with the idea that *Cryptosporidium* is only distantly related to Coccidia and probably more closely related to gregarine protozoa (Leander *et al.*, 2003). Phylogenetic reconstructions do not support the monophyly of *Cryptosporidium*. Instead, these studies suggested that *Cryptosporidium* forms an independent evolutionary lineage as an early branching clade at the base of the apicomplexans (Zhu *et al.*, 2000). Although highly controversial at this time, a new class termed Cryptosporidae has been proposed (Slapeta, 2007).

Cryptosporidium taxonomy and the naming of species have undergone rapid changes due to the collaboration of classical descriptive techniques and new PCR based molecular methods. Originally, oocyst morphology, the anatomical site of infection and an isolate's host specificity were the criteria used for classification (Fayer and Ungar, 1986). Although morphology remains an integral method for classification

and naming species, more current molecular techniques and DNA analysis are usually required. Currently, there are 16 described species of *Cryptosporidium* from a wide array of hosts including mammals, reptiles, and fish. Of these, *C. parvum* has the widest host range (although still limited to mammalian hosts) and displays the greatest intra-specific variability. There are 21 genotypes of *Cryptosporidium parvum* currently recognized (Chacin-Bonilla, 2007; Ryan *et al.*, 2008).

III ULTRASTUCTURE

All developmental stages in *Cryptosporidium* were studied in detail by light-, transmission electron-, and scanning electron-microscopy, as well as by other techniques. Morphological knowledge is crucial for understanding the uniqueness of this parasite.

All apicomplexans possess a group of organelles for host cell invasion at the anterior end of sporozoites called the **apical complex** (Fig. 1). This complex is present only in the motile cell invasive stages of the parasite, typically the sporozoites and merozoites (Blackman and Bannister, 2001). The apical organelles (rhoptries, micronemes, dense granules) are secretory vesicles that take part in cell adhesion and entry into the host cell (micronemes), formation of a parasitophorous vacuole (rhoptries), modifying the host cell after invasion (dense granules), and enabling the gliding motility of the parasite (micronemes). The content of the apical complex differs between the species and genera. *Cryptosporidium* has only one rhoptry, but multiple micronemes and dense granules (Chen *et al.*, 2004).

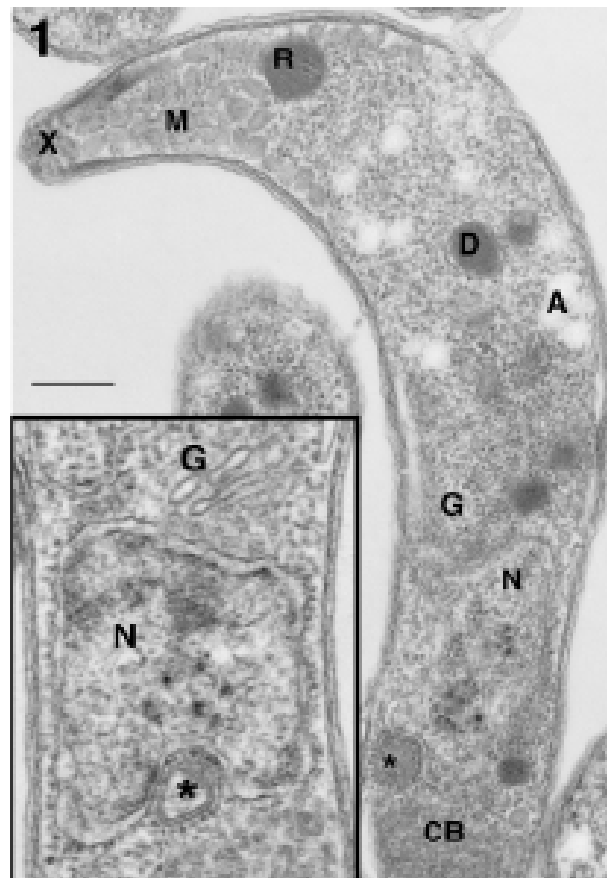
Cryptosporidium has highly reduced **mitochondrion** without cristae and with rather expanded internal compartments. It is located in between the nucleus and a crystalloid body (Fig. 1) (Keithly *et al.*, 2005). The existence of the *Cryptosporidium* mitochondrion was not recognized for a long time by transmission electron microscopists. The organelle observed next to the nucleus was considered to be an apicoplast (remnant plastid) that is present in other apicomplexans (Tetley *et al.*, 1998). However, genome sequencing of *C. parvum* and *C. hominis* confirmed that

both species of *Cryptosporidium* lack apicoplast genes (Abrahamsen *et al.*, 2004; Xu *et al.*, 2004). Furthermore, both species do contain several genes with N-terminal mitochondria targeting sequences including an alternative oxidase (AOX) (Roberts *et al.*, 2004), chaperonin 60 (Riordan *et al.*, 2003) and heat shock protein 70 (HSP70) (Slapeta and Keithly, 2004). However, none of the mitochondrial genes for oxidative phosphorylation are present, which is reflected in the overall reduced size of the organelle and by the absence of mitochondrial cristae which are associated with ATP generation (Xu *et al.*, 2004). In contrast to other apicomplexans, *Cryptosporidium* does not possess a mitochondrial genome, and all mitochondrial genes are encoded by the nucleus (Abrahamsen *et al.*, 2004). The discovery that several genes encoding mitochondrial-type iron-sulphur clusters (IscS, IscU) are targeted to this organelle suggests a possible reason for retaining this relict organelle (LaGier *et al.*, 2003).

An additional organelle, the **crystalloid body** (CB), can be observed in the close apposition to the relict mitochondrion as well as to the nucleus. This organelle was described in Archicregarines (species *Selenidium*), a sister group to *Cryptosporidium* (Schrével, 1971). The CB is at least equal in volume to that of the nucleus, but despite its large volume, its function is still unknown. Initial electron tomographic reconstructions revealed that the closely packed membrane vesicles of the CB may be interconnected, but additional research is needed to resolve this question, as well as whether a limiting membrane surrounds this organelle (Keithly *et al.*, 2005). Experiments with mitotracker vital dyes (Mitotracker Green FM, Rhodamine B, Rhodamine 123) revealed that both the CB and mitochondrion exhibit a membrane potential (Citrnacta *et al.*, 2006).

Many **granules made of amylopectin** are dispersed throughout the cytoplasm of *Cryptosporidium*. These granules are present in different life stages of the parasite and are used as a carbohydrate storage (Harris *et al.*, 2004).

Figure 1. Transmission electron microscopy of a *C. parvum* sporozoite. The mitochondrion (*) is located between the nucleus (N) and crystalloid body (CB). There is a typical apical complex (X) with micronemes (M), one rhoptry (R) and dense granules (D). A Golgi complex (G) is located next to nucleus. Amylopectin granules for carbohydrate storage (A) are dispersed through the sporozoite.



IV THE LIFE CYCLE

A monoxenous life cycle is typical for species of *Cryptosporidium*, meaning that the parasite can complete its entire life cycle within a single host. The *C. parvum* life cycle (Fig. 2) occurs within the host gastrointestinal tract, and begins with the ingestion of mature sporulated oocysts. Once in the gastrointestinal tract, changes in temperature, pH, and the presence of bile salts and pancreatic enzymes trigger

excystation which results in the release of four motile infective sporozoites from the oocyst (Reduker *et al.*, 1985). Free sporozoites then actively invade the surrounding intestinal epithelial cells.

Internalization and localization of sporozoites within the microvilli of the host cell is a unique process. **Internalization** starts with the attachment of the sporozoite to the apical membrane of a host epithelial cell via the apical complex of the parasite. The single rhoptry of the parasite is recruited and extends to the attachment site, followed by secretion of microneme and dense granule enzymes forming several vacuoles at the parasite-host membrane interface (Huang *et al.*, 2004). It is at this location that an actin-containing electron-dense band is established, termed the feeder organelle, which directly separates the parasite from the host cell cytoplasm (Elliott and Clark, 2000). Simultaneously, *Cryptosporidium* invasion induces host cell membrane protrusions along the edge of the host-parasite interface which leads to the parasite being enveloped by the host cell plasma membrane. This process eventually results in a mature parasitophorous vacuole (PV) containing the parasite within the host cell but outside the host cell cytoplasm. This intracellular but extracytoplasmic localization enables the parasite to both develop and be protected from the host immune system and extracellular environment (Lumb *et al.*, 1988). Although PVs were observed in other apicomplexans, including *Plasmodium* (Ladda *et al.*, 1969) and *Eimeria* (Jensen and Edgar, 1976), that of *Cryptosporidium* is unique because of its localization at the apical site of the host cell rather than deep within the cytoplasm.

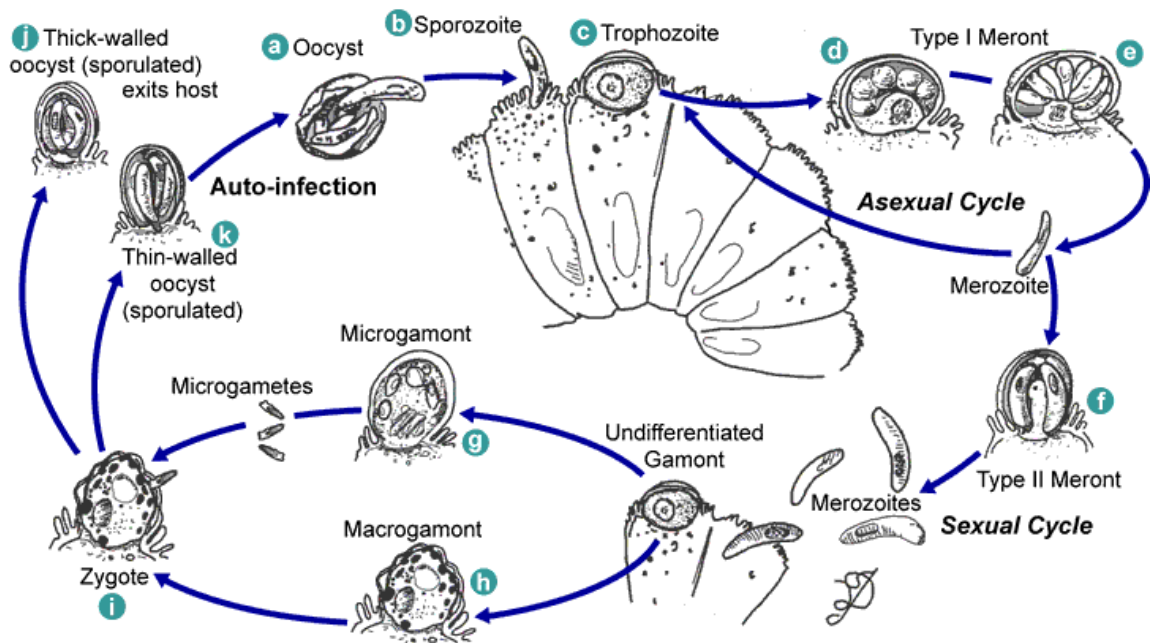
Within the cell, *Cryptosporidium* undergoes asexual and sexual reproduction. During the **asexual reproduction** (Carey *et al.*, 2004) the sporozoite differentiates into a trophozoite that divides and gives rise to 1st generation (type I) meronts – a process known as merogony. Type I meronts contain eight small oval merozoites (Hijjawi *et al.*, 2004), which actively invade other epithelial cells to undergo a second round of merogony. This usually results in the production of type II meronts containing four merozoites. Alternatively, instead of developing into type II meronts, the first-round merozoites can form more type I meronts. This feature is thought to be partially

responsible for the common autoinfection that occurs with *Cryptosporidium* infection.

Type II merozoites then further develop into gamonts through a process known as gamogony. During **gamogony** (Current and Garcia, 1991) these second-stage merozoites infect other epithelial cells in order to produce microgamonts or macrogamonts. The macrogamont is extracytoplasmic and contains only one macrogamete, whereas the microgamont will undergo several rounds of division producing 16 motile microgametes. These microgametes bud from the surface of microgamonts and are subsequently released into the intestinal lumen.

A microgamete will fuse with a macrogamete to yield a zygote which undergoes **sporogony**, the only sexual stage of the life cycle. Upon fertilization, the macrogamont divides twice to develop into an oocyst with four naked and infectious sporozoites. During sporogony, both thin-walled and thick-walled oocysts are formed. About 20% of oocysts are thin-walled, surrounded only by a thin single membrane. These oocysts are not able to survive environmental conditions, and remain within the host causing additional rounds of autoinfection, which can be very detrimental for immunocompromised individuals. Approximately 80% of the oocysts formed are thick-walled. The thick wall consists of an outer layer of acidic glycoproteins, an intermediate layer of elastic glycolipid/lipoprotein material and a thick inner glycoprotein filamentous layer (Carey *et al.*, 2004). Thick-walled oocysts are excreted in the feces are fully-infectious, requiring no external maturation.

Figure 2. The life cycle of *Cryptosporidium parvum*.



V CRYPTOSPORIDIOSIS

Outbreaks and routes of transmission of cryptosporidiosis

Cryptosporidium has become increasingly recognized as a pathogen responsible for outbreaks of diarrheal illnesses in both immunocompetent and immunocompromised persons. Infection is thought to occur primarily through ingestion of water contaminated with oocysts. To date, at least 325 major **water-associated outbreaks** due to parasitic protozoans have been reported worldwide, and *Cryptosporidium parvum* accounts for the majority of them (165; 50.8%) (Karanis *et al.*, 2007). Because *Cryptosporidium* oocysts are chlorine-resistant, the outbreaks are often associated with recreational water (Insulander *et al.*, 2005) or water parks (Wheeler *et al.*, 2007) and can be a particular threat to otherwise safe drinking water supplies. In the USA, the parasite was identified in more than 95% of all surface waters

(LeChevallier *et al.*, 1991). Several cases of contaminated municipal water supply systems were reported, even though in some cases the water met all state and federal safety standards. The most significant outbreak occurred in Milwaukee, Wisconsin, USA, in April 1993, when an estimated 400,000 people were sickened resulting in the death of more than 100 immunocompromised individuals (MacKenzie *et al.*, 1995).

While not as widespread as waterborne transmission, **foodborne *Cryptosporidium* transmission** has been documented. For example, in 1993 in the USA, an outbreak of cryptosporidiosis (154 cases) was due to drinking unpasteurized fresh-pressed apple juice. The apples were most likely contaminated by cattle feces when they fell to the ground in a cow pasture (Millard *et al.*, 1994).

Person-to-person transmission has been documented in outbreaks among close social groups such as households, nurseries and hospitals. In nurseries, infants are clustered together as they share play areas and can be easily infected, as well as employers who change diapers. In an outbreak at a day-care center in the USA, 49% of the center's 79 children and 13% of its 23 staff became infected with *Cryptosporidium* through person-to-person transmission (Tangermann *et al.*, 1991). Cryptosporidiosis can be also transmitted during sexual practices, especially among homosexuals (Hellard *et al.*, 2003).

Zoonic transmission is a well established mode of transmission. Many sporadic cases of cryptosporidiosis are due to human contact with infected farm animals (Feltus *et al.*, 2006). For example, cryptosporidiosis among calves was transmitted to 11 of 19 (58%) infants and young children 10 to 15 months old, and three of 27 children in a closed agricultural community (Miron *et al.*, 1991).

Global distribution of cryptosporidiosis

Both human and animal cryptosporidiosis has been identified on all continents. It has been predominantly caused by two main species: *C. parvum* and *C. hominis*.

C. parvum is typically found in Europe and England and has the widest host specificity, whereas *C. hominis* is responsible for 62% of cryptosporidiosis in North America, South America, Australia and Africa (Caccio *et al.*, 2005). In addition to these, 5 other species: *C. maleagridis*, *C. canis*, *C. felis*, *C. suis* and *C. muris* are known to cause human disease. These *Cryptosporidium* species have different animal reservoirs including cattle, mice, pigs, goats, horses, turkeys, cats, dogs, deer, monkeys, human and others (Guyot *et al.*, 2001; Xiao *et al.*, 2001; Gatei *et al.*, 2003).

The prevalence of cryptosporidiosis is higher in developing countries; mainly due to the lack of clean water and sanitary facilities, crowded housing conditions and large numbers of domestic animals near homes (potential reservoir hosts). In these countries *Cryptosporidium* infection is diagnosed up to 37% of those with gastrointestinal complaints (Tumwine *et al.*, 2005), whereas cryptosporidial infections in individuals with diarrhea in industrialized countries is about 2.9% (Horman *et al.*, 2004). There is a significantly greater prevalence in children (Samie *et al.*, 2006) which also correlates with the warmer and wetter months (Wongstitwilairoong *et al.*, 2007). However, these studies are always difficult to compare because studied populations may not be identical or different stool sampling and oocyst detection methods are used. Additionally, many laboratories do not routinely test stool specimens for *Cryptosporidium* unless specifically requested, resulting in significant underreporting of disease among the immunocompetent population.

The prevalence of cryptosporidiosis in immunocompromised patients was previously very high but cryptosporidiosis among HIV/AIDS patients in developed countries has significantly decreased due to the routine use of Highly Active Anti-Retroviral Treatment (HAART) which began in the late 1990s. For example, one study reported a prevalence of 20% among HIV-positive patients in 1994, which had fallen to 6% by 1998 (Inungu *et al.*, 2000). However, in developing countries the prevalence of cryptosporidiosis among HIV/AIDS patients is still as high as 63% due to the high cost of antiretroviral treatment (Adjei *et al.*, 2003).

Human cryptosporidiosis in the Czech Republic

Both in Europe and in the Czech Republic, the prevalent species of *Cryptosporidium* in humans is *C. parvum*. A genotyping study identified *C. parvum* as the only strain in isolates from a limited number of Czech children (Hajdusek *et al.*, 2004). In another study from South Bohemia, *C. parvum* was detected in 5.8% of children aged 2 – 36 months and hospitalized with acute diarrhea (Chmelik *et al.*, 1998). These clinical findings are also reflected in the environmental detection of *Cryptosporidium* oocysts in fresh water sources. Even though the numbers of *Cryptosporidium* oocysts were elevated up to 7400 oocysts per 100 l in one water reservoir after floods in 1997, and a relatively high number of *Cryptosporidium* oocysts was found in treated water, no waterborne *Cryptosporidium* outbreak has been reported to date (Dolejs *et al.*, 2000). The absence of outbreaks in the Czech Republic has been attributed to a strong serological response against *Cryptosporidium*-specific antigens by 33% - 72% of the population from four different parts of the Czech Republic. The strong serological response of the population indicates previous contact with *Cryptosporidium*, which could result in protective immunity for cryptosporidiosis. This might be the reason why no waterborne outbreaks were reported (Kozisek *et al.*, 2007). The national reference laboratory in Prague has been reporting individual cases of cryptosporidiosis (Table 1), but cryptosporidiosis in the Czech Republic is underreported. The majority of cases occur in small children and the cause of diarrhea is not always diagnosed.

Table 1. Incidence of cryptosporidiosis among patients in the Czech Republic. Data provided by Dr. Tolarova from the national reference laboratory in Prague.

Year	2000	2001	2002	2003	2004	2005	2006	2007
<i>Cryptosporidium parvum</i>	5 and 1 import	9	12	7	5	5	5	7

VI OOCYSTS AND WATER TREATMENT

Oocysts and their resistance to common infectants

Species of *Cryptosporidium* are distributed worldwide, which is largely due to the infective thick-walled oocysts that are very stable in an environment. Oocysts are commonly found in surface and ground water (Lisle and Rose, 1995), soil (Anguish and Ghiorse, 1997), sea water (Johnson *et al.*, 1997) and even in swimming pools (Insulander *et al.*, 2005). The survival of oocysts ultimately depends on the outdoor conditions. Oocysts of *C. parvum* can retain infectivity in 15 °C **fresh water** up to seven months (Jenkins *et al.*, 2003), and 6 - 8 °C **sea water** for as long as 12 months. Even though dilution of the sea is enormous and the risk of oocyst ingestion for swimmers is very low, the oocysts can be concentrated during water filtration on the **gills of mussels** and be a potential danger for gourmands who eat them uncooked. As few as 10 oocysts from gill washings were determined to be infective in neonatal BALB/c mice (Tamburrini and Pozio, 1999).

Infected people and animals can pass up to 10 billion *C. parvum* oocysts per gram of feces (O'Handley *et al.*, 1999). Therefore, only a few animals (or humans) can contaminate large quantities of water. Because vehicles of environmental contamination include agricultural runoff as well as sewage effluent, the survival of oocysts in human and bovine feces and in **soil** was previously studied. After 176 days, 44 % of *C. parvum* oocysts in feces at ambient temperatures were still viable (Robertson *et al.*, 1992). From - 4 to 4 °C, the oocysts could survive in water and soil for >12 weeks, but degradation was accelerated both at 25 °C and in feces or soil containing natural microorganisms. It was suggested that after at least 12 weeks of storage contaminated cattle feces should be distributed on fields during warmer weather to reduce the potential of waterborne transmission following heavy rainfalls that result in agricultural runoffs (Olson *et al.*, 1999).

Extreme temperatures, as well as desiccation are critical for the viability of oocysts (Fayer, 1994). At high temperatures (> 64 °C for 5 min), the oocyst wall is disrupted

by denaturation of oocyst wall proteins, exposing sporozoites to a hostile environment. Both rapid freezing in liquid nitrogen and desiccation for 2 h inactivates 100 % of oocysts. However, slow freezing, which occurs naturally during environmental stress, is less effective in killing the oocysts. After 152 hours at -22°C, 10% of oocysts remained viable (Robertson *et al.*, 1992).

Infectivity

Very small numbers of infectious, viable thick-walled oocysts excreted into the environment are sufficient to cause infection. Studies performed on healthy volunteers showed that the median infective dose for either *C. parvum* (DuPont *et al.*, 1995) or *C. hominis* (Chappell *et al.*, 2006) was 132 oocysts (minimum 30) or 83 oocysts (minimum 10), respectively. However, it was shown that only a single oocyst can produce infection and disease in susceptible hosts (Pereira *et al.*, 2002). The infectivity of *Cryptosporidium* also varies within isolates of a single species (Okhuysen *et al.*, 1999). It has been suggested that when 10-30 oocysts of *Cryptosporidium* per 100 l in treated water is detected, preventive actions against an outbreak of cryptosporidiosis should be taken (Haas, 2000).

Water treatment

Cryptosporidium oocysts are resistant to most **disinfectants and antiseptics**. Exposure to undiluted household **bleach** (5%) for 30 minutes lowers viability only by 7% (Deng and Cliver, 1999). Even **chlorination**, the method most commonly used by water treatment plants to cleanse water of potentially harmful pathogens, will not kill oocysts. They are resistant at concentrations significantly higher than that commonly used for water treatment (Korich *et al.*, 1990). *Cryptosporidium* oocysts are more resistant to chlorination than cysts of other prevalent waterborne microorganisms, for instance *Giardia intestinalis*, which accounts for 40.6% (132 of 325) of parasitic disease outbreaks (Karanis *et al.*, 2007).

There are two effective treatments that lead to damage of *Cryptosporidium* oocysts; **ozone** (Peeters *et al.*, 1989) and **ultra-violent light** (Craik *et al.*, 2001). Although these techniques are very expensive and cannot safeguard the water against additional exposure that may occur as the water moves beyond the treatment facility and further along the distribution chain.

The traditional physical removal of particles is an important step in treating drinking water. The improved **micro-filtration system** is able to reduce the risk of oocysts appearing in the drinking water supply. However, outbreaks have more often been associated with filtered water than unfiltered water. Pathogens and other debris were concentrated on the filters and after a breakthrough in the filters there was a local increase in the number of oocysts in the water resulting in an increased risk of infection. These filtration failures are usually due to operational problems of water treatment plants rather than inherent treatment deficiencies (MacKenzie *et al.*, 1995).

Studies from the USA and Spain showed that even after water plant treatment in industrialized countries the drinking water still contain a small number of oocysts (LeChevallier *et al.*, 1991; Carmena *et al.*, 2007). Thus for prevention, immunocompromised patients are recommended to use portable filters to avoid potential infection or boil the water for at least one minute. Both *C. parvum* and *C. hominis* usually pass through most conventional filters with a pore size of 8 - 10 μm . Specialized reverse-osmosis portable water filters or filters which are designed to remove parasites (*Giardia/Cryptosporidium*) have an "absolute" pore size of 0.1 – 1 μm , and therefore, may also remove most diarrhea-causing bacteria (CDC: Preventing cryptosporidiosis). These filters can be used by travelers in areas where tap water is not chlorinated or where sanitation is poor.

VII HUMAN DISEASE

Clinical manifestation

Clinical symptoms typically appear within seven days after the ingestion of *Cryptosporidium* oocysts (Jokipii and Jokipii, 1986). They include a profuse watery diarrhea without the presence of blood or leukocytes. Other less common clinical features are nausea, vomiting, abdominal cramps and occasionally fever. Dehydration and weight loss result directly from the symptoms.

The course of the infection largely depends upon the immune status of a patient. Infection in **immunocompetent individuals** usually lasts for two weeks or less, although during that time clinical symptoms might improve and then worsen. Occasionally, the illness may last for more than two weeks, or the infection can be asymptomatic. Cryptosporidiosis in immunocompetent hosts is usually self-limited and results in spontaneous, complete recovery (Current and Garcia, 1991).

People with severely weakened immune systems, **immunocompromised**, such as AIDS patients, the elderly or organ transplant recipients often have great difficulty in clearing the parasite. They often suffer a more severe diarrhea that can last long enough to become life threatening (Colford, Jr. *et al.*, 1996). The cholera-like fluid loss in patients with AIDS can be as much as 17 l of watery stool per day. In severe cases, the parasite can spread to other parts of the body such as the lungs, stomach, biliary tract or pancreas (Clark, 1999). In cases where suppression of the immune system cannot be reversed, symptoms may persist until death.

Pathogenesis and immunology of the disease

Studies in neonatal mice, calves and pigs have increased our understanding of the course of infection in humans (Farthing, 2000). The infection moves from the proximal to distal end of the intestinal tract where intestinal enterocytes are infected and damaged by the invasion of parasites. This includes the displacement of the

microvillus brush border causing villi shortening and crypt hyperplasia occurs. Thus, the intestinal surface area is decreased, membrane-bound digestive enzymes are lost, and nutrient and electrolyte transport is impaired (Chen *et al.*, 2002). The malabsorption may result in subsequent overgrowth of intestinal microflora, change in osmotic pressure across the gut wall and an influx of fluid into the lumen of the intestine. While the infection in the small intestine often leads to severe diarrhea, infections in the distal ileum, large intestine and pyloric region of the stomach are usually asymptomatic. Occasionally, the gastric mucosa, bile duct, gall bladder and respiratory epithelium are also infected (Thompson *et al.*, 2005).

Both humoral and cell-mediated immune responses are involved in parasite elimination. The most important role is that of a **cell-mediated immune response** by CD4⁺ T cells - especially intraepithelial lymphocytes and their production of IFN- γ . This interferon induces host enterocyte resistance to parasite invasion. Humans and animals without a sufficient number of CD4⁺ T cells are unable to clear *Cryptosporidium* infection. CD8⁺ T cells are important later during recovery from the infection (Deng *et al.*, 2004).

During infection, the **humoral immune response** develops. Although both serum and mucosal antibodies are elevated, their protective role is unclear at this time. Parasite-specific immunoglobulin A (IgA) antibody responses have been demonstrated in animals and humans without parasite elimination (Dann *et al.*, 2000). However, it has been shown that passive immunization using IgG polyclonal antibodies derived from the sera or colostrum of immunized cattle reduced oocyst shedding and clinical signs both in experimental and natural infections of animals (Doyle *et al.*, 1993). Thus, a search for immunogenic antigens of *Cryptosporidium* was initiated, and a number of them associated with parasite motility, attachment, invasion and development were subsequently identified (Sibley, 2004). Monoclonal antibodies to some of these antigens were produced and tested for protection against cryptosporidiosis, but in most cases *Cryptosporidium* infection was only reduced and not eliminated (Riggs *et al.*, 2002). The polyvalent neutralizing antibodies were shown to provide better protection than monoclonal antibodies (Thompson *et al.*,

2005). However, an effective vaccine against *Cryptosporidium* is still not available.

Diagnosis

Most laboratories do not test for *Cryptosporidium* unless requested by a physician. Parasites are typically identified by microscopic examination of the stool where the most simple method of detecting oocysts is by modified acid-fast staining (Milacek and Vitovec, 1985). Many other tests with a different range of sensitivity and specificity can be used. These include immunochromatic tests (Crypto-strips), immunofluorescent microscopic assays (direct fluorescent antibody), enzyme immunoassay (ELISA), agglutination assays, molecular PCR-based techniques or usage of histological detection. Serological tests are of limited value because many healthy persons have antibodies against *Cryptosporidium* (Chen *et al.*, 2002).

Therapy

Before the introduction of **HAART** in the 1990s, cryptosporidiosis was an important cause of morbidity and mortality in AIDS patients (Chen *et al.*, 2002). This therapy helps improve the immune status of the patients and is why the prevalence of AIDS-related opportunistic infections connected with low CD4⁺ cell counts has been significantly reduced. Still, cryptosporidiosis remains among the most common causes of diarrhea in patients with AIDS (Morpeth and Thielman, 2006).

Interestingly, most of the chemotherapeutic agents effective against coccidian parasites and other apicomplexans are ineffective against cryptosporidiosis. Although the overall treatment for *Cryptosporidium* is still unsatisfactory, one promising drug has been “rediscovered”: **nitazoxanide** (NTZ, a 5-nitro-2-thiazolylbenzamide derivate). This compound was originally developed for the treatment of intestinal helminthic infections (Rossignol and Maisonneuve, 1984) and in 2002, became the first Food and Drug Administration (FDA)-approved medication for treating cryptosporidiosis in American children. There were several encouraging results in clinical trials. These randomized, double-blind placebo-controlled studies in children

and immunocompetent adults treated with NTZ at 8 mg per kg twice daily for three days or 500 mg doses twice daily for three days, respectively reduced both the duration of diarrhea and oocyst shedding (Rossignol, 2006). The same course of treatment also reduced mortality among the malnourished young children with cryptosporidiosis (Amadi *et al.*, 2002). Another study involving AIDS patients also produced remarkable results. Of the patients evaluated, 66% responded to NTZ and most of them within the first two weeks of therapy. Although this study showed that doses of 3,000 mg per day may be safely administered, the optimum recommended dose was 1,000 mg per day. Two weeks of treatment were generally sufficient for patients with $> 50 \text{ CD4}^+$ cells/mm³, while at least eight weeks of treatment were required for patients with $< 50 \text{ CD4}^+$ cells/mm³ (Rossignol, 2006).

In Europe, NTZ has not yet been approved for use in humans. Thus the drug of choice is paromomycin or azithromycin. **Paromomycin** (PRM, an aminoglycoside antibiotic) has been tested in double-blind placebo-controlled trials of adults with AIDS exhibiting $< 150 \text{ CD4}^+$ cells/mm³. In these studies, PRM was no more effective than the placebo. However, when combined with interleukin (IL)-12 PRM appeared to act synergistically against *C. parvum* infection, and up to 73% of mice infected with the parasite were cured from infection (Gamra and el-Hosseiny, 2003). Remarkable results were also obtained in a small open trial in which PRM was combined with **azithromycin** (a macrolide antibiotic). A significant reduction of clinical symptoms in AIDS patients with $< 100 \text{ CD4}^+$ cells/mm³ was observed when they were treated with both drugs for four weeks, and then with PRM alone for an additional eight weeks (Smith *et al.*, 1998).

Although passive immunotherapy and some chemotherapeutic agents (e.g. PRM or NTZ) improve clinical signs and symptoms, none of these completely clear the patient of *Cryptosporidium*. Most of these agents do not eliminate the parasite from the host, but simply reduce oocyst shedding and improve clinical well-being (Thompson *et al.*, 2005). The treatment of immunocompetent patients is usually limited to **supportive care** (fluid replacement, careful hygiene), since there are no specific and safe anticryptosporidial medications. If a safe and effective therapy were

available most clinicians would probably treat severe acute diarrheal illness with it.

VIII GENOME

The *C. parvum* (Abrahamsen *et al.*, 2004) and *C. hominis* (Xu *et al.*, 2004) genome projects have provided us with the valuable clues to the complicated biology of *Cryptosporidium*. It was found that the *Cryptosporidium* genome is relatively small and compact: the 9.1 Mbase genome is distributed into eight chromosomes. When compared to its *P. falciparum* relative, the *Cryptosporidium* genome is 2.5 times smaller (Gardner *et al.*, 2002). This difference is due to the lack of both the apicoplast and mitochondrial genomes, as well as an absence of many nuclear genes that function in these organelles. In addition, *Cryptosporidium* contains coding sequences containing relatively few introns and is almost devoided of repetitive DNA, and its genes are smaller in overall size than those in *P. falciparum*. It is estimated that about 3,800 predicted proteins are encoded by the *C. parvum* genome. This implies that many biochemical pathways are streamlined or completely absent. For example, the degeneration of the mitochondrion and a lack of enzymes for the Krebs cycle suggest that the parasite relies solely on glycolysis for energy production. Enzymes required for the fatty acid oxidative pathway are also absent, indicating that fatty acids are apparently not an energy source (Abrahamsen *et al.*, 2004).

On the other hand, a significant number of genes appear to have been acquired by lateral gene transfer (LGT) from bacteria and by duplication events. *Cryptosporidium* also possess several “plant-like” enzymes that are either absent in mammals or highly divergent, and these may be essential to the parasite. Acquired enzymes seem to contribute to the extreme parasitic adaptation and display specific enzymatic activities and metabolic processes that are distinct from those in mammals, providing unique opportunities for chemotherapy (Thompson *et al.*, 2005).

IX BIOCHEMICAL PROCESSES

The fate of glucose

With the loss of almost all mitochondrial functions, *Cryptosporidium* is incapable of completely oxidizing substrates to carbon dioxide and water. There is no electron transport-linked ATP-generation. Instead, this parasite relies upon cytosolic substrate-level phosphorylation during fermentative glycolysis for energy production (Entrala and Mascaro, 1997).

Glucose, as well as its oligomers and polymers, serve as carbohydrate sources of energy for *Cryptosporidium*. The parasite has the capacity to transport and then metabolize monosugars (glucose, fructose) as well as to store, synthesize and catabolize carbohydrate polymers (e.g. amylopectin, trehalose). The plant-like branched polymer of glucose, amylopectin, is the main energy storage granule seen throughout the cytoplasm in *Cryptosporidium* (Harris *et al.*, 2004). *C. parvum* can utilize amylopectin to produce glucose-1-phosphate via glycogen phosphorylase. It has been shown that sporozoites depleted of amylopectin exhibited decreased infectivity for host cells *in vitro* (Fayer *et al.*, 2000). Unlike most amitochondrial protists, the nucleus of *Cryptosporidium* does not encode glycerol kinase so no glycerol is produced (Thompson *et al.*, 2005). Although *Cryptosporidium* can utilize maltose (a dimer of glucose), its activity is quite low in *C. parvum* oocyst homogenates (Entrala and Mascaro, 1997). The absence of most of enzymes of the pentose phosphate pathway, β -oxidation and for catabolism of proteins suggests that amino acids, nucleotides and lipids do not support energy metabolism (Xu *et al.*, 2004).

Both homogenates of *C. parvum* oocysts and sporozoites display activities for nearly all glycolytic enzymes (Entrala and Mascaro, 1997). The step-wise conversion of glucose to fructose-6-phosphate is similar to that of other eukaryotes. It is at this point that core carbohydrate metabolism diverges among mammals and microaerophilic protists. Like other amitochondrial protists, *Cryptosporidium* uses

inorganic pyrophosphate (PP_i) instead of ATP in some glycolytic reactions. The assumed physiological significance of this substitution is a decreased investment of ATP with an overall increase in ATP production. *C. parvum* utilizes **PP_i linked phosphofructokinase** (PP_i-PFK), a plant-like enzyme different from human ATP-dependent phosphofructokinase (Denton *et al.*, 1996; Abrahamsen *et al.*, 2004). This enzyme catalyzes the phosphorylation of fructose-6-phosphate to fructose-1,6-bisphosphate, and spares the consumption of ATP during glycolysis, so the overall yield of ATP per glucose is three rather than two molecules. This increase is critical for anaerobic protists relying only on substrate-level phosphorylation. Consecutive reactions lead to the production of **phosphoenolpyruvate**, which is a branch site for the formation of pyruvate that is synthesized primarily by ADP-dependent pyruvate kinase (Denton *et al.*, 1996). There is an alternative pathway to pyruvate formation in which oxalacetate is carboxylated and then reduced by malate dehydrogenase to malate. Malate decarboxylase can then decarboxylate malate to yield pyruvate (Thompson *et al.*, 2005).

Glycolysis in *Cryptosporidium* results in the production of three well-known end products: lactate, acetate and ethanol (Abrahamsen *et al.*, 2004). The final product depends upon the initial glucose concentration. If glucose is in excess, pyruvate can be converted to lactate or ethanol to regenerate NAD⁺. **Lactate** is formed in one step from pyruvate using an α -proteobacterial type **lactate dehydrogenase** (LDH) which has been characterized (Zhu and Keithly, 2002; Madern *et al.*, 2004).

Ethanol may be produced by two independent pathways, either from pyruvate or from acetyl-CoA. In the first pathway, pyruvate is catabolized first by a decarboxylase and then a monofunctional alcohol dehydrogenase (ADH). In the second pathway, ethanol is produced from acetyl-CoA by a typical prokaryotic bifunctional **alcohol/acetaldehyde dehydrogenase** (AdhE), which also is observed in the anaerobic protists *Giardia* and *Entamoeba*, but not other apicomplexans (Dan and Wang, 2000).

Under glucose-limiting conditions, conversion of acetyl-CoA to **acetate** occurs

through the action of an ADP-forming acetyl-CoA synthetase (ACS) in substrate level phosphorylation (Abrahamsen *et al.*, 2004).

The fate of pyruvate

The most significant divergence of amitochondrial organisms from those with a mitochondria is in the mechanism of oxidative decarboxylation of pyruvate to acetyl-CoA, a central step of core energy metabolism. All organisms with an aerobic mitochondria utilize the **pyruvate dehydrogenase complex** (PDH), which consists of the stepwise transfer of electrons via an acetyl group to CoA, then from dihydrolipoamide to FAD, and finally to NAD⁺. Under anaerobic conditions, pyruvate is usually converted into lactate and ethanol.

In amitochondrial anaerobic protists, two distinctly different enzymatic systems for metabolizing pyruvate have evolved. Both of them are oxygen sensitive and function only under anaerobic conditions. One is **pyruvate formate lyase** (PFL) present in facultatively anaerobic eubacteria and some microaerophilic unicellular eukaryotes (e.g. *Escherichia coli*). Flavodoxins or ferredoxins serve as electron acceptors for PFL in *Euglena* or *Clostridium* (Gelius-Dietrich and Henze, 2004). The other system occurs in anaerobic prokaryotes and microaerophilic eukaryotes including *Trichomonas vaginalis*, *Entamoeba histolytica*, and *Giardia intestinalis*. The enzyme responsible for oxidative decarboxylation in these organisms is the iron-sulphur protein, **pyruvate ferredoxin oxidoreductase** (PFO), which converts pyruvate to acetyl-CoA with the transfer of a pair of electrons to ferredoxin. PDH and PFO are not homologous enzymes, i.e. both localization and utilization of cofactors differ (Muller, 2003).

In contrast to all other anaerobic protists and prokaryotes, *Cryptosporidium* utilizes a unique enzyme for oxidative decarboxylation, **pyruvate-NADP oxidoreductase** (PNO) containing an N-terminal pyruvate:ferredoxin oxidoreductase domain fused with a C-terminal NADPH-cytochrome P450 reductase (CPR) domain (Rotte *et al.*, 2001). Such a PFO-CPR fusion has been previously observed only in the

euglenozoan protist *Euglena gracilis* (Inui *et al.*, 1987), and was also recently detected in the genome of the centric diatom *Thalassiosira pseudonana* (Ctrnacta *et al.*, 2006). In *E. gracilis* PNO catalyzes both a reversible pyruvate oxidation by NADP⁺ and a pyruvate CO₂ exchange, similar to the reactions catalyzed by PFO. However, unlike PFO, the PNO of *Euglena* does not react with ferredoxin.

Fatty acid synthesis

Unlike *Cryptosporidium*, other apicomplexans (*Plasmodium*, *Toxoplasma*, and *Eimeria*) possess a relict chloroplast, an apicoplast, that contain a plant-like type II fatty acid synthase for the *de novo* synthesis of fatty acids. These enzymes consist of discrete monofunctional proteins for fatty acid synthesis (Goodman and McFadden, 2007). Because *Cryptosporidium* lacks an apicoplast, the pathway for type II fatty acid synthesis is also lacking (Zhu, 2004). Instead, *C. parvum* possess a cytosolic giant **type I fatty acid synthase** (CpFAS1), and is the only FAS in this parasite. CpFAS1 is a multifunctional protein consisting of 21 enzymatic domains that function in the elongation of fatty acids using medium to long chain fatty acids as precursors. The absence of a type II fatty acid synthase and the presence of a single type I FAS incapable of using short-chain fatty acids as loading units indicates that *Cryptosporidium* is unable to synthesize fatty acids *de novo* (Zhu *et al.*, 2004). In addition to CpFAS1, a **type I polyketide synthase** (CpPKS1) has been discovered (Zhu *et al.*, 2002). The biosynthesis mechanisms of both type I PKSs and FASs are nearly identical. Some polyketides serve as medically important antibiotics, antitumor agents and immunosuppressive molecules (Staunton and Weissman, 2001). Genes for CpFAS1 and CpPKS1 together comprise more than 0.5% of the entire *C. parvum* genome (Abrahamsen *et al.*, 2004). Their presence indicates that *C. parvum* may have the capacity to elongate medium-chain fatty acids or saturated and unsaturated long-chain fatty acids and polyketides, instead of salvaging them from the intestine of the host.

In addition to CpFAS1 and CpPKS1, a number of other enzymes involved in fatty acid metabolism have also been identified. These include a long chain fatty acyl elongase (CpLCE1), a cytosolic acetyl-CoA carboxylase (ACCase), three acyl-CoA synthetases (ACS), and an unusual "long-type" acyl-CoA binding protein (ACBP). However, *C. parvum* lacks enzymes for the oxidation of fatty acids, indicating that fatty acids are not an energy source for this parasite (Fritzler *et al.*, 2007; Zhu, 2004).

Nucleic acid synthesis

All enzymes for the *de novo* synthesis of nucleic acids in are absent in *Cryptosporidium*. This parasite depends upon nucleic acid transport from the host for both purine and pyrimidine salvage. Consistent with the lack of *de novo* synthesis for pyrimidines, *C. parvum* lacks the entire pentose phosphate pathway. *C. parvum* purine metabolism has been reduced to include only a few enzymes. Among the retained enzymes are adenosine kinase and enzymes catalyzing the conversion of AMP to IMP, XMP and GMP. All of the enzymes necessary to produce ATP, GTP, dATP and dGTP from adenosine are present in the genome (Thompson *et al.*, 2005). One of these enzymes, IMP dehydrogenase (IMPDH), is believed to have been acquired by horizontal gene transfer from an ϵ -prokaryote, and has been characterized and investigated as a potential drug target (Umejiego *et al.*, 2004; Umejiego *et al.*, 2008).

In contrast to *Cryptosporidium*, all other apicomplexans have retained a synthetic pathway for the *de novo* synthesis of pyrimidines. An algal-type uracil phosphoribosyltransferase and uracil kinase, as well as a bacterial thymidine kinase acquired by horizontal transfer compensate for the loss of this pathway in *Cryptosporidium* (Donald and Roos, 1995). None of these three enzymes, which enable the parasite to produce UTP, CTP, TTP and dCTP from uracil, have been detected in other apicomplexans (Striepen *et al.*, 2004). Nucleic acid transporters for uracil, uridine, cytosine and adenosine have also been identified in the *Cryptosporidium* genome (Abrahamsen *et al.*, 2004).

Amino acid synthesis

Cryptosporidium, like other anaerobic parasites, lives in an amino acid-rich environment, and relies upon uptake from the host using a set of at least 11 **amino acid transporters** (Abrahamsen *et al.*, 2004). It has been suggested that the *Cryptosporidium* genome once contained genes for the biosynthesis of all amino acids but has lost the ability to synthesize most of them. Although *Cryptosporidium* has maintained the ability to synthesize a few selected amino acids, most of these pathways are coupled with the generation of co-factors for other reactions. The retained amino acid synthetic pathways include those for asparagine, glutamine, glycine and proline (Payne and Loomis, 2006). Because *C. parvum* also lacks the recycling enzymes methionine synthetase and methylene-tetrahydrofolate reductase, it is suspected that methionine is obtained from the host cell. (Thompson *et al.*, 2005).

Methionine cycle and polyamine biosynthesis

Most intracellular methionine is converted into S-adenosylmethionine (AdoMet) by S-adenosyl-L-methionine synthase (SAMS). AdoMet is an integral part of the methionine cycle included in sulphur-containing amino acid metabolism (Nozaki *et al.*, 2005). It is a major methyl donor in *C. parvum* as AdoMet donates its methyl moiety to almost all known biological methylation reactions except for the reactions involved in methylation of homocysteine. In humans, it has been estimated that about 95% of AdoMet is consumed in the methyl transfer reactions (Mudd and Pool, 1975). The methionine cycle is regulated through **S-adenosylhomocysteine hydrolase** (SAHH). *C. parvum* SAMS and SAHH have been both characterized and display significant differences from mammalian homologues. They are being studied as potential drug targets (Slapeta *et al.*, 2003; Ctrnacta *et al.*, 2007).

The remainder of AdoMet is interconnected closely with **polyamine metabolism**. Polyamines are biologically active triamines that include putrescine, spermidine and spermine. These polyamines play a key role in controlling important biological processes such as regulation of transcription and translation of many genes,

modulation of enzyme activities, regulation of ion channels, and the regulation of posttranslational modification (Bacchi and Yarlett, 2002). Their necessity has been demonstrated by elevated levels of polyamines in rapidly growing cells (Pegg, 1988). In *Cryptosporidium*, polyamine metabolism differs from its host but resembles that of plants and some bacteria. Data from the genome sequencing project revealed that polyamine metabolism is probably reduced as genes for several key enzymes have not been identified (e.g. AdoMet decarboxylase, spermine synthase, methionine synthase). The lack of spermine synthase indicates that spermine is salvaged from the host cell, and corresponds to fact that the very active back-conversion pathway from spermine to spermidine is present in *C. parvum*. This pathway might be more essential for salvaging polyamines than the biosynthetic forward pathway (Bacchi and Yarlett, 2002).

In mammalian cells, and the majority of protozoa, synthesis of polyamines occurs by the decarboxylation of ornithine to putresceine by ornithine decarboxylase (Yarlett, 1988). In *C. parvum* arginine, rather than ornithine, is utilized by arginine decarboxylase, agmatine iminohydrolase and N-carbaminoputresceine amidohydrolase to produce putresceine. The forward pathway from putresceine to spermine is present in most eukaryotes. AdoMet serves as a substrate in the production of decarboxylated AdoMet, which is further utilized for the formation of spermidine from putresceine. Although no AdoMet decarboxylase gene has been identified in *C. parvum*, its activity has been detected in sporozoites (Keithly *et al.*, 1997).

AIMS OF THE DISSERTATION

This dissertation builds on a long term research goal of our laboratory. The focus of our laboratory is to characterize the molecular and biochemical features of enzymes involved in the core metabolism of *Cryptosporidium parvum* in an effort to characterize a new drug targets for novel therapeutics development.

The specific objectives of the research described in this dissertation are following:

- To determine the subcellular localization of one of the core metabolic enzymes, pyruvate:NADP⁺ oxidoreductase, which is responsible for converting pyruvate to acetyl-CoA.
- To characterize a *Narf*-like gene in *Cryptosporidium* that resembles [Fe]-hydrogenases in other anaerobic protists and to explore this unique gene as a potential drug target.
- To characterize S-adenosylhomocysteine hydrolase from *C. parvum*. This is an important enzyme regulating the S-adenosylhomocysteine metabolic pathway considered important in the target-based drug design of antiviral and antiparasitic drugs.
- To validate adenosine analogues capable inhibiting both the recombinant enzyme S-adenosylhomocysteine hydrolase and *in vitro* growth of *C. parvum*.

Objectives are dealt with in individual chapters where the research results are described in detail.

METHODS

I ORGANISMS

Following organisms were used in the course of described studies:

Euglena gracilis - culturing

Euglena gracilis strain B without a plastid was originally obtained from the Pasteur Institute in Paris, France and subcultured at the Faculty of Sciences, Charles University in Prague, Czech Republic. The culture medium L25 for *Euglena* consists of 2 g sodium acetate, 1 g proteose peptone in 1 l of distilled water, pH 6.0. Cells were grown aerobically in the dark at 20°C. After centrifugation, cells were washed in PBS and immediately frozen in liquid N₂ and later used for western blot assay.

Cryptosporidium parvum

C. parvum (Iowa strain) was isolated from calves at Bunch Grass Farms, Drury, ID, USA. All oocysts examined were less than three months old since the time of harvest from infected calves. Upon arrival to our laboratory, oocysts were Clorox-treated, PBS-washed and purified by CsCl gradient centrifugation (Zhu and Keithly, 1997).

The excystation of sporozoites was performed for 1 h at 37 °C in Hanks' balanced salt solution (HBSS) containing 0.25% trypsin and 0.75% taurodeoxycholic acid (Zhu and Keithly, 1997). Sporozoites were used immediately for DNA and RNA isolation, microscopy or frozen in PBS at -80 °C for western blots.

The human colorectal cell line HCT-8 – culturing and parasite infection

The host cells used for *C. parvum* infection were HCT-8 cells (ATCC CCL-244). They were seeded at a concentration of 1.0×10^5 per well in a 48-well plate format. Cells were grown overnight until they reached ~80% confluency at 37°C, in 5% CO₂, in RPMI 1640 medium (Sigma) containing 10% fetal bovine serum (FBS), 15 mM HEPES and other supplements (Cai et al. 2004, Upton et al. 1995).

Host cells were infected with 10-fold serial dilutions of *C. parvum* oocysts with host-cell to parasite ratios ranging from 2:1 to 20,000:1 (= 50,000 to 5 oocysts per well) to generate standard curves. The drug testing procedure included 5,000 oocysts per well, and parasites were incubated for 4 h at 37 °C to allow enough time for excystation and invasion into host cells. At this time an exchange of culture medium (described above, containing drug or control media with no drug) was performed to remove parasites that failed to infect the host cells. The drugs used in this study were S-DHPA, R-DHPA, EritA (all provided by Prof. Antonin Holy, Institute of Organic Chemistry and Biochemistry, Academy of Sciences of the Czech Republic) and Ara-A (Sigma). Stock solutions of S-DHPA, R-DHPA, EritA were dissolved in water, and Ara-A was dissolved in dimethyl sulfoxide (DMSO). Drugs were then added to the infected cultures at various concentrations during the medium exchange. Cultures were then allowed to incubate at 37°C in 5% CO₂ for 44 hours. Each drug concentration was assayed in at least duplicates, and each experiment was repeated at least three times.

***Escherichia coli* – culturing**

E. coli TB1 cells (New England Biolabs) were used as a background organism for MBP-SAHH expression. TB1 cells with the construct were preincubated overnight in 3 ml LB medium with 0.2% glucose and 100 µg/ml ampicillin at 37°C. Overnight culture was added into fresh medium and was grown until the OD₆₀₀ reached ~ 0.5.

II NUCLEIC ACID METHODS

Library screening, subcloning, sequencing

A gene fragment similar to [Fe]-hydrogenases of anaerobic protists (gn1/CVMUMN 5807/ cparvum contig 2535) was identified by BLAST search using an *Entamoeba histolytica* [Fe]-hydrogenase query. This *C. parvum* fragment was PCR-amplified, random-primer labeled with [α -³²P]-dATP and used as a probe for library screening.

Gene fragment similar to SAHH of anaerobic protists was identified within the *C. parvum* genome sequence survey (GSS) (Strong and Nelson, 2000). The corresponding plasmid was obtained from Dr. R. Nelson, University of California, San Francisco, CA, USA. This insert was completely sequenced and was used as a radioactively labeled probe for library screening.

The complete open reading frames for both genes were deduced from sequences of overlapping clones isolated from *EcoRI* and *HindIII* *C. parvum* gDNA libraries constructed in pBluescript SK⁺ (Stratagene). The amplified full-length genes were cloned into the pCR2.1 TOPO vector (Invitrogen). They were sequenced on both strands to confirm their identities. Both genes were submitted to the GeneBank under accession numbers AY145118 (CpNARF) and AY161083 (CpSAHH).

Alignments and phylogenetic analysis

The recovered DNA sequences of *CpNARF* and *CpSAHH* were translated to amino acids. Multiple protein sequence alignments of both CpNARF and CpSAHH with their homolog proteins from different taxa were created (Clustal X program, PAM 250 amino acid matrix) and related proteins compared. The conservative or active residues were identified.

A total of 292 amino acid positions of putative CpNARF protein including the H-cluster domains and one neighboring iron-sulfur ([4Fe-4S]) cluster were used to

calculate trees in three different phylogenetic programs. Both a maximum likelihood (ML) tree analysis using WAG+ Γ + θ model of amino acid evolution (1,000 quartet puzzling values) and a likelihood mapping analysis (10,000 values) were performed using the TREE-PUZZLE v. 5.0 program. A Bayesian phylogenetic search for tree space using a variant of the Markov Chain Monte Carlo (MCMC) was performed in the MrBayes 2.01 program. Metropolis-coupled MCMC analysis used the JTT+ Γ + θ model of amino acid evolution.

DNA and RNA isolation

Total genomic DNA (gDNA) and RNA were isolated from *C. parvum* sporozoites and from mock-infected HCT-8 cells, as well as from cultures infected with *C. parvum*. For isolation, DNA Mini Kit (Qiagen) and RNeasy Mini Kit (Qiagen) were used according to manufacture's instructions.

Southern blot

For Southern blot analysis of *CpNARF* and *CpSAHH* genes, total gDNA was isolated from *C. parvum* sporozoites. The gDNA was digested with *EcoRI* or *HindIII*, separated by electrophoresis and transferred to Zeta-probe Nylon membranes (Bio-Rad). [α - 32 P]-dATP random-primer-labeled DNA fragment of the *CpNARF* or *CpSAHH* gene was used to probe blots under conditions of high stringency (Sambrook and Russel, 2001).

RT-PCR analysis for gene expression

Total RNA was isolated from *C. parvum* sporozoites, from mock-infected HCT-8 cells, as well as from HCT-8 infected with *C. parvum*. The first strand cDNA was synthesized from DNase treated RNA (SuperScript First-Strand Synthesis for RT-PCR), using a *CpNARF*-specific reverse primer or a *CpSAHH*-specific reverse primer. Further, PCR amplification used gene-specific primer pairs either *CpNARF*-F, *CpNARF*-R or *CpSH*-F, *CpSH*-R. Identity of the RT-PCR products was confirmed

by sequencing.

qRT-PCR

Total RNA was isolated from infected cultures 44 h after infection using an RNeasy RNA isolation kit (Qiagen). RNA concentration and quality from each sample were determined by measuring their absorbances at 260 and 280 nm, and all RNA samples were adjusted to 20 ng/μl. Both parasite 18S rRNA and human 18S rRNA were detected via qRT-PCR using the following primers: Cp18S-1011F (5' TTG TTC CTT ACT CCT TCA GCA C 3'), Cp18S-1185R (5' TCC TTC CTA TGT CTG GAC CTG 3'), Hs18S-1373F (5' CCG ATA ACG AAC GAG ACT CTG G 3'), and Hs18S-1561R (5' TAG GGT AGG CAC ACG CTG AGC C 3'). Each of these primers has been widely used by our laboratory and others in detecting Cp18S rRNA and Hs18S rRNA. A SYBR green-based real-time RT-PCR method was employed using the QuantiTect SYBR Green RT-PCR kit (Qiagen). Reactions contained 20 ng of total RNA. Appropriate amounts of reagents and primers were first incubated at 48°C for 30 min to synthesize cDNA, heated at 95°C for 15 min to inactivate the reverse transcriptase, and then subjected to 40 thermal cycles (95°C for 20 s, 50°C for 30 s, and 72°C for 30 s) of PCR amplification with an iCycler iQ real-time PCR detection system (Bio-Rad). At least two replicate reactions were performed for each sample. Analysis of Cp18S rRNA and Hs18S rRNA levels and the eventual calculations of parasite inhibition were calculated (Cai et al. 2005).

III PROTEIN METHODS

Cloning and expression of *pMAL-CpSAHH*

The full-length *CpSAHH* sequence was PCR amplified from *C. parvum* gDNA using sense F1 and antisense R1 primers. Gel-extracted amplicons of *CpSAHH* were ligated into the polylinker cloning site of the pMAL-c2x vector (New England Biolabs) cleaved with *Bam*HI and *Pst*I. The *pMAL-SAHH* construct was transformed to *E. coli* TB1 cells. Plasmids isolated from transformed cells were subjected to

restriction analyses and subsequently sequenced to confirm their identities before expression. Expression of the MBP-CpSAHH was induced with 0.3 mM IPTG for 15 h at 30°C.

Purification of pMAL-CpSAHH

Cells expressing MBP-CpSAHH were harvested by centrifugation, and resuspended in column buffer (20mM Tris-HCl, 200mM NaCl, 1mM EDTA, pH 7.2). After sonication on ice, bacteria were centrifuged to pellet cell debris. The MBP-CpSAHH fusion protein was affinity purified using amylose resin-based chromatography according to the manufacturer's instructions (New England Biolabs). Protein concentration was estimated using the Bradford assay with bovine serum albumin (BSA) as a standard. The identity of MBP-CpSAHH was confirmed by SDS-PAGE and western blotting. Aliquots of protein were stored at -20°C and used either for the SAHH assay or were cleaved with Factor Xa to release the MBP tag.

Cleavage of MBP-CpSAHH with Factor Xa

A reaction mixture of the fusion protein and 1.5% Factor Xa was incubated in a column buffer with 10 mM maltose for two days at 4°C. After cleavage, this buffer was replaced by a 20 mM sodium phosphate buffer, pH 7.2, and concentrated using an Amicon Centricon ultrafilter with 30 kDa cutoff (Millipore).

Purification of CpSAHH on hydroxyapatite column and determination of its size

The concentrated sample was applied to a CHT 5-I hydroxyapatite column, equilibrated with 20 mM sodium phosphate buffer. The CpSAHH protein was then eluted over a linear gradient from 0 - 1 M sodium phosphate buffer, pH 7.2. Fractions containing purified CpSAHH were subjected to SDS-PAGE and stained with Coomassie blue. Aliquots of protein were stored at -20°C and were later assayed for SAHH activity. The size of the active recombinant SAHH enzyme was analyzed

under native conditions by size exclusion column chromatography (Superdex 200 10/300 GL column).

SAHH activity assay

The enzymatic activities of both the MBP-CpSAHH fusion protein and cleaved CpSAHH were spectrophotometrically assayed in the hydrolytic direction (Yuan *et al.*, 1996; Lozada-Ramirez *et al.*, 2006) using S-adenosylhomocysteine as a substrate. During the catalytic conversion of S-adenosylhomocysteine by CpSAHH, adenosine and L-homocysteine are formed, and the concentration of L-homocysteine is measured using 5,5'-dithiobis (2-nitrobenzoic acid) (DNTB = Ellman's reagent). The extinction coefficient of $13,600 \text{ M}^{-1}\cdot\text{cm}^{-1}$ for 5-thio-2-nitrobenzoate (TNB), the product of the DNTB reaction, was used to calculate the amount of L-homocysteine formed. Adenosine deaminase was used in the assay to ensure that the reaction proceeds in the hydrolytic direction by converting adenosine to inosine. The reaction mixture contained various concentrations of S-adenosylhomocysteine (0.8–100 μM), 4U Ado deaminase, 250 μM DNTB in 50 mM potassium phosphate buffer with 1 mM EDTA, pH 7.2. CpSAHH was added just before assaying activity at 412 nm, 37°C in a Shimadzu UV 601 spectrophotometer. Control reactions contained all components except the enzyme. The measurements were repeated at least four times, and one unit of enzyme activity was defined as the amount of protein catalyzing the consumption of 1 μM of TNB per minute.

SAHH inhibition assay

Inhibition assays were carried out by the preincubation of 5 μl of 500 $\mu\text{g/ml}$ CpSAHH with different concentrations of Ara-A, S-DHPA and D-eritadenine for 15 min at 37°C. After incubation SAHH activity was assayed by adding 50 μM S-adenosylhomocysteine at a final volume of 1 ml to start the reaction. The same experiment was repeated four times with different inhibitor concentrations: 0, 10, 100, 500 nM and 1 μM .

Western blot

Sonicated sporozoite extract and extract from *E. gracilis* trophozoites were subjected to SDS-PAGE and then transferred to a nitrocellulose membrane. Both primary polyclonal antibodies against PFO and CPR domains (prepared using synthetic oligopeptides) were used to reveal the expression of the complete PNO protein in *C. parvum* and *E. gracilis*. The membrane was blocked, incubated with the primary antibodies overnight at 4°C, washed and incubated for 1 h with horseradish peroxidase-conjugated immunoglobulin G: either with 1:10,000 anti-rabbit, or 1:2,000 anti-goat secondary conjugate (Bio-Rad and Invitrogen, respectively). The membrane was finally washed and blots were visualized using the ECLTM Western Blotting Analysis System (Amersham Biosciences).

Peptide competition assay for specificity of antibodies

As a control of antibody specificity, a peptide competition assay was employed. The oligopeptide used for producing antibody was preincubated with the appropriate antibody. Specificity was evaluated and confirmed by the lack of a signal on the western blot due to antibody interaction with the oligopeptide leaving no antibody to bind on the nitrocellulose membrane. The negative control included the preincubation of heterologous oligopeptides with the antibody in which case the signal on western blot should be detected.

IV MICROSCOPY: LOCALIZATION

The polyclonal primary antibodies against both the PFO and CPR domains of CpPNO were prepared using synthetic oligopeptides in a rabbit and a goat by ProSci Inc. Poway, CA, USA. As a control, a primary antibody against cytosolic fatty acid phosphopantetheinyl transferase (CpPPT) was used. CpPPT was a gift from Dr. Guan Zhu (Texas A&M University, College Station, TX, USA). Another control antibody against *C. parvum*-specific mitochondrial heat shock protein CpCpn60 was provided by Dr. Jan S. Keithly (Wadsworth Center, Albany, NY, USA).

Confocal microscopy

Freshly excysted sporozoites were fixed in 4% (w/v) paraformaldehyde, permeabilized using 0.2% (v/v) Triton X-100 in PBS, blocked with 5% (w/v) BSA in PBS and single or double stained with primary antibody (anti-PFO, anti-CPR, anti-CpPPT or anti-CpCpn60) at 4°C overnight. After washing with PBS, secondary fluorescent antibodies were subsequently applied for 1 hour. The nucleus was labeled with DAPI. For visualization of the mitochondrion, fresh living sporozoites were stained with MitoTracker Green FM for 30 minutes. After washing, slides were mounted using a Slow Fade Light antifade kit (Molecular Probes), and were examined with a Zeiss LSM 510 confocal microscope.

Transmission electron microscopy

Freshly excysted sporozoites were fixed in methanol-free 4% (v/v) formaldehyde (Polysciences) and embedded in LR White (Riordan *et al.*, 2003). Semi thin sections were blocked for 30 min in a solution containing 20 mg/ml BSA in TBS (containing 20mM Tris, 0.1% BSA, 0.05% Tween-20, 150mM NaCl, 20mM NaN₃, pH 7.4), single or double stained (anti-PFO, anti-CPR, anti-CpPPT or anti-CpCpn60) at 4°C overnight. After being washed the sections were labeled for 1 h with a 1:100 dilution of TBS containing 10 mg/ml reconstituted whole goat serum and to which one or two of the following EM-grade secondary antibody gold conjugates had been added: 10-nm gold particles conjugated to goat anti-rabbit IgG antibodies, 6-nm gold particles conjugated to donkey anti-goat IgG antibodies and/or 15-nm gold particles conjugated to donkey anti-rabbit IgG antibodies. Sections were then washed in TBS, exposed to 1% (v/v) glutaraldehyde in water for 5 min to covalently link the primary antibody to the secondary one, stained with 2% (w/v) aqueous uranyl acetate for 20 min, and finally washed three times in water. For negative controls, primary antibodies were replaced by TBS. Sections were examined at 80 and 120 kV with a Zeiss 910 transmission electron microscope.

The materials and methods were described in details in the published articles entitled: “Localization of Pyruvate:NADP⁺ Oxidoreductase in Sporozoites of *C. parvum*” (Citrnacta *et al.*, 2006); “A *Narf*-like gene from *C. parvum* resembles homologues observed in aerobic protists and higher eukaryotes” (Stejskal *et al.*, 2003); “Characterization of S-adenosylhomocysteine hydrolase from *C. parvum*” (Citrnacta *et al.*, 2007). The methods that have not been published yet are described in details in this chapter.

RESULTS AND DISCUSSIONS

I LOCALIZATION OF PYRUVATE: NADP⁺ OXIDOREDUCTASE (PNO) IN SPOROZOITES OF *Cryptosporidium parvum*

PNO in *Euglena gracilis* mitochondrion

Pyruvate:NADP⁺oxidoreductase (PNO) is a rare fusion of an N-terminal pyruvate:ferredoxin oxidoreductase domain (Fe-S protein) fused with a C-terminal NADPH-cytochrome P450 reductase domain (flavodoprotein). An activity of complete PNO fusion was firstly described in the flagellated photosynthesing protozoan *Euglena gracilis*. It was shown that *E. gracilis* PNO (EgPNO) is able to catalyze the oxidative decarboxylation of pyruvate with NAD⁺ as the electron acceptor (Inui *et al.*, 1984; Inui *et al.*, 1987). The EgPNO was isolated from the *E. gracilis* mitochondria which are unique facultatively anaerobic organelles that produce ATP in the presence and absence of O₂ (Rotte *et al.*, 2001). Aside from EgPNO, the mitochondria also contain functional subunits of pyruvate dehydrogenase (PDH) typical for aerobic metabolism. **Under anaerobic conditions**, pyruvate is decarboxylated to acetyl-CoA by EgPNO which serves as a building unit for the synthesis of fatty acids and wax esters. The stored waxes are degraded via aerobic dissimilation in mitochondrion after the return to aerobic conditions (Inui *et al.*, 1987). **In the presence of O₂**, both EgPNO and PDH are expressed and acetyl-CoA is produced, even though the expression of EgPNO is significantly lower compared to the expression under anaerobic conditions and compared to the PDH expression (Hoffmeister *et al.*, 2004). The resulting acetyl-CoA then enters a modified citric acid cycle and respiratory chain (Rotte *et al.*, 2001). Thus, oxidative decarboxylation, via PFO as a domain of PNO, is coupled with a Krebs cycle. The simultaneous presence of PNO and PDH in the mitochondria and its ability to function both under aerobic and anaerobic conditions indicate that this organelle in *E. gracilis* is unique in that it unites biochemical properties of aerobic and anaerobic

mitochondria and hydrogenosomes.

PNO from *Cryptosporidium parvum*

In *C. parvum*, a PFO-like fragment was identified in the genome (Liu *et al.*, 1999) and after cloning and sequencing the entire gene, it was found that it consists of two domains as in *E. gracilis*. PNO is the only enzyme that is capable of direct converting pyruvate to acetyl-CoA in *C. parvum*. Because *Cryptosporidium* relies solely on glycolysis as an energy source, CpPNO might play a crucial role in the carbohydrate metabolism. This role and the absence of PNO in mammalian cells suggest this enzyme is a potential drug target.

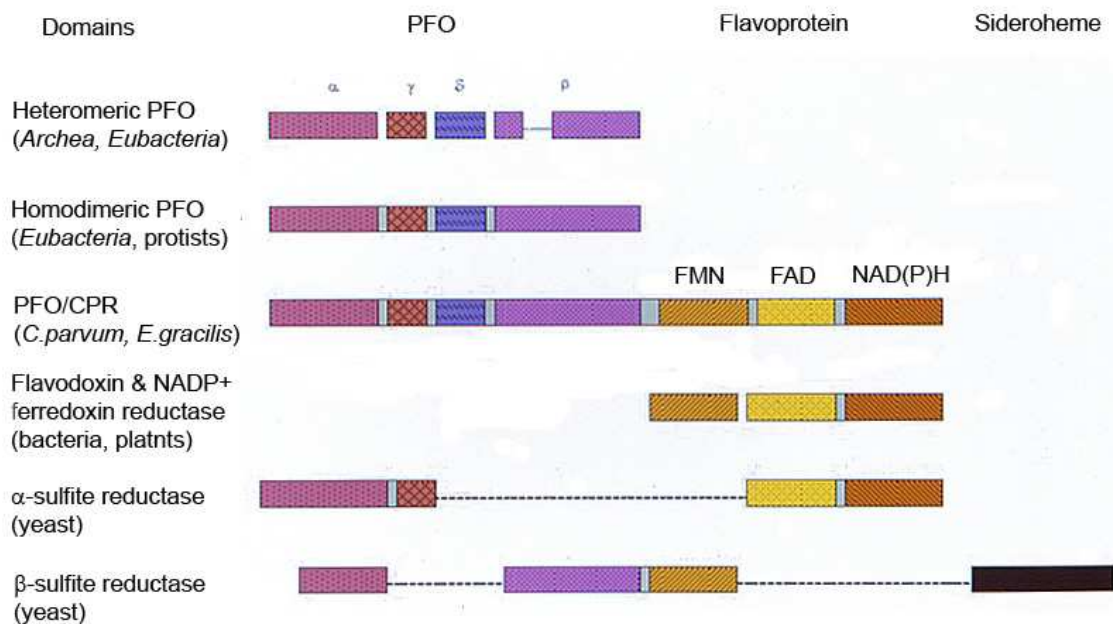
Southern blot analysis showed that PNO is a single copy gene (Rotte *et al.*, 2001), which was later confirmed by whole genome sequencing (Abrahamsen *et al.*, 2004). The PNO expression profile was determined with RT-PCR analysis, and gene expression was identified to occur both in sporozoites and in the intracellular stages. Multiple sequence analysis of CpPNO, EgPNO and other prokaryotic and eukaryotic PFO and CPR homologues indicated that CpPNO contained most of the amino acid residues and motifs necessary for enzymatic activities. However, its exact enzymatic function and its localization in *C. parvum* remained unclear (Rotte *et al.*, 2001).

PNO, its fragments and evolution

Complete PFO-CPR fusions have been previously observed only in the Euglenozoan protist *E. gracilis* (Inui *et al.*, 1987) and in *C. parvum* (Rotte *et al.*, 2001). All fusions contain a PFO domain and a CPR domain with FMN, FAD and NADP subdomains (Fig. 3). EgPNO and CpPNO are 40% identical in their amino acid sequences and share 30%-35% amino acid identity with eukaryotic and eubacterial PFOs, but only 20%-25% identity with archaeobacterial PFOs. There is only 25% identity of the FMN subdomain between CpPNO CPR and EgPNO CPR. No archaeobacterial homologue of CPR was found (Rotte *et al.*, 2001). Incomplete PNO fusions were found in yeast as part of the sulfite reductase α and β subunits (Hansen *et al.*, 1994). It is possible

that these sulfite reductase subunits are the result of the reduction and the gene fragmentation of the same ancestral PNO as in CpPNO and EgPNO.

Figure 3. The module organization of *C. parvum* PFO/CPR gene and its prokaryotic and eukaryotic homologues.



Wide phylogenetic analysis of PFO or PNO proteins suggests that the common ancestor of diplomonads, trichomonads, *Entamoeba*, euglenids, apicomplexans and fungi possessed the same inherited eubacterial PFO gene. Similar to PFO, PNO seems to have been acquired only once and early in the evolutionary process (Rotte *et al.*, 2001). However, PFO subdomain in EgPNO probably functions differently from the other PFOs that are present in anaerobic organisms because unlike other PFOs, PNO enzyme from *Euglena* does not react with ferredoxin (Rotte *et al.*, 2001).

It is well-established that the PFO of certain parasites can be either cytosolic (e.g. in *G. intestinalis*, *Entamoeba histolytica*) or organellar (e.g. in *T. vaginalis*, *Nyctoterus ovalis*) within double membrane bounded hydrogenosomes (Boxma *et al.*, 2005;

Muller, 2003). To clarify whether CpPNO is localized primarily within the cytosol or within the relict mitochondrion, *C. parvum* sporozoites were analyzed by confocal immunofluorescence and transmission electron microscopy (TEM) and the results are described in this dissertation.

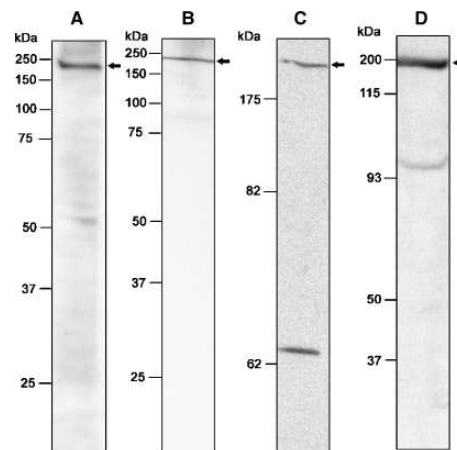
Results

Using parasite-specific anti-CpPFO and anti-CpCPR antibodies, **the presence of CpPNO in *C. parvum* sporozoites** was confirmed by western blotting (Fig. 4). Amino acid sequence analysis revealed that CpPNO is structurally similar to EgPNO as they share significant sequence homology and domain organization. However, their function and localization are not identical. No CpPNO activity in *C. parvum* sporozoites was detected, in spite of detectable EgPNO activity in the *E. gracilis* positive control (Hrdy, Stejskal, Ctrnacta, unpublished results). The forward reaction of this enzyme was assayed using pyruvate as an electron donor, and methyl violagen, NADP⁺, NAD⁺ or FAD as electron acceptors (Inui *et al.*, 1987). The reverse reaction in *C. parvum* was assayed using methods well-established for *E. gracilis*, clostridia and photosynthetic bacteria (Inui *et al.*, 1987). Positive controls included both mitochondrial EgPNO and the hydrogenosomal *Trichomonas vaginalis* PFO. It is difficult to learn why CpPNO, but not its activity, is present in sporozoites without an efficient *in vitro* *Cryptosporidium* cultivation system. The quantity of CpPNO may be below the detection limits of our enzymatic assays in sporozoites, or the functional protein may only be expressed by intracellular stages multiplying in the intestinal epithelium under microaerophilic conditions, similar to that for the PFO of diplomonads, entamoebids and trichomonads. It is also possible that the biochemistry of this organism is so different that assay systems currently used for detection of the PFO or PNO activities in other organisms are deficient in some essential cofactor required by *C. parvum*.

Despite we have not managed to detect any activity, it is assumed that PNO might be responsible for the transfer of electrons to NTZ leading to the drug activation and formation of toxic metabolites. It is suspected that in *C. parvum*, a more significant

domain might be the PFO domain of CpPNO, which might activate NTZ in a manner similar to anaerobic protists and bacteria. It is assumed that the 5-nitro group of NTZ is reduced by PFO. This reduction could result in the formation of nitro-radical forms that bind to DNA and cause their breakage (Coombs and Muller, 2002). However, on the contrary, another report claims that NTZ could be activated by cytochrome P450 domain of CpPNO (Coombs and Muller, 2002).

Figure 4. Western blot analyses of sonicated extracts from *Cryptosporidium parvum* and *Euglena gracilis*, respectively. The arrows designate the position of the PNO protein. Lane A. Goat anti-CpPFO recognizes a 217-kDa CpPNO band in *C. parvum* sporozoites. Lane B. Rabbit anti-CpPFO recognizes an identically sized band in *C. parvum* sporozoites. Lane C. Rabbit anti-CpCPR recognizes both a 217-kDa band and an additional 75-kDa band in *C. parvum* sporozoites (probably *C. parvum* cytochrome P450 reductase-like protein, CpCPR2). Lane D. Cross-reactivity: rabbit anti-CpPFO also recognizes a ~200-kDa EgPNO band in *Euglena gracilis*.



As previously described, CpPNO is phylogenetically related to the PFO of anaerobic protists and it is well established that the PFO of these parasites can be either cytosolic or organellar (Embley *et al.*, 2003). It was determined that EgPNO is localized in *E. gracilis* mitochondrion (Inui *et al.*, 1984). Whereas EgPNO apparently contains a signal peptide sequence to the mitochondrion, no signal peptide sequence was identified in CpPNO (Rotte *et al.*, 2001). These data are consistent with the idea that the mitochondrial targeting presequence of CpPNO might have been secondarily lost in this apicomplexan lineage during the reductive evolution of its mitochondrion (Williams and Keeling, 2003), and that the enzyme subsequently became cytosolic

(Rotte *et al.*, 2001). Before this study, the possibility that CpPNO could still be targeted to its relict mitochondrion by an alternative mechanism could have not been excluded. It is known that some mitochondrial proteins have internal import signals and that N-terminal targeting sequences may be lacking, especially in proteins involved in electron transport in lower eukaryotes (Emanuelsson and von Heijne, 2001; Henriquez *et al.*, 2005).

By confocal immunofluorescence and TEM it has been shown that **CpPNO is localized within the cytosol rather than within the relict mitochondrion** (Fig. 5 - 8). *C. parvum* specific polyclonal antibodies against CpPFO, the cytosolic CpPPT, and the mitochondrial CpCpn60 were used for co-localization and TEM experiments. The absence of CpPNO in the *C. parvum* relict mitochondrion supports the suggestion that the relict mitochondrion primarily serves as an organelle for the import and maturation of Fe-S clusters (Keithly *et al.*, 2005).

Interestingly, both immunofluorescence and TEM experiments showed that **CpPNO is also localized in the crystalloid body (CB)** - an organelle whose function is currently unknown (Fig. 6 - 8, 11 - 14). The size of the CB is significant as it is at least equal in volume to the nucleus. The 3-D reconstruction of this organelle indicates that the closely packed vesicles observed by TEM might be a series of interconnected channels. This organelle is always closely positioned to the relict mitochondrion, outer nuclear membrane and rough-endoplasmic reticulum (Keithly *et al.*, 2005). Even though there were no clear observations of limiting membrane made, it was shown that the CB takes up MitoTracker Green FM dye, suggesting there is some kind of membrane, possibly with an organellar membrane potential (Fig. 9, 10). Recently, the refractile bodies (RB) in *Eimeria tenella* have been characterized (de Venevelles P. *et al.*, 2006). Both RBs and the CB are differentially expressed during the life cycle of the parasites (both organelles are found only in sporozoites and type I meronts). After invasion, these organelles disappear, and reappear only in newly shed oocysts. It has been suggested that RBs contain numerous proteins and lipids that might play a part during invasion process (deVenevelles P. *et al.*, 2006). The function of the CB in *C. parvum* might be

consistent with RBs in *E. tenella*. Furthermore, CpPNO localization within the CB may indicate the presence of additional ATP generation to power the invasion of the parasite to the host cell.

Figure 5 - 8. Confocal microscopic immunolocalization of pyruvate:NADP⁺ oxidoreductase (CpPNO) in *Cryptosporidium parvum* sporozoites. Scale bars - 5 μ m. 5. Control localization of cytosolic fatty acid phosphopantetheinyl transferase (CpPPTase) using Alexa-488 donkey anti-rabbit secondary antibody shows diffuse green fluorescence throughout the cytoplasm. 6. Using Alexa-633 donkey anti-goat secondary antibody against goat IgG anti-CpPFO, both the CpPNO in the cytosol and the crystalloid body (arrows) exhibit red fluorescence. 7. The sporozoites are stained with Alexa-488 donkey anti-rabbit secondary antibody against rabbit IgG anti-CpPFO. The same pattern of the fluorescence in both the cytosol and crystalloid body (CB) is seen in Fig. 6. The arrows show the posterior region where the CB is situated. The nucleus is stained with DAPI (blue). 8. When Fig. 5 and Fig. 6 are merged, co-localization of CpPNO and CpPPTase within the cytosol is observed (yellow). The higher concentration of CpPNO within the crystalloid body (red) is readily apparent. The nucleus is stained with DAPI (blue).

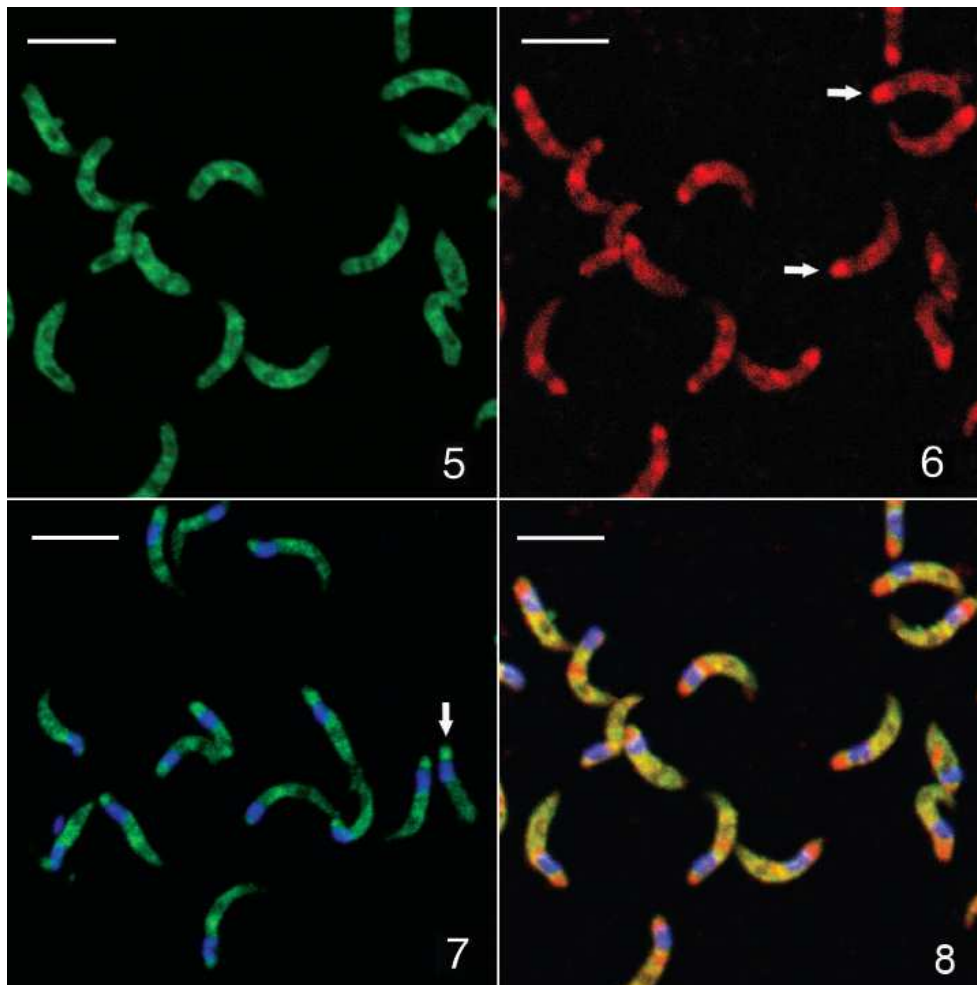


Figure 9 - 10. The uptake of MitoTracker Green FM into the mitochondrion and crystalloid body of *Cryptosporidium parvum* sporozoites. Scale bars - 5 μm . 9. Dye uptake indicates the presence of an organellar membrane potential. Because of the close juxtaposition of these two organelles, and the small size of the mitochondrion, the fluorescence of individual mitochondria separate from the crystalloid bodies cannot be determined. 10. Phase contrast image of the same sporozoites showing the anterior (A) and posterior (P) of an individual sporozoite (arrows). The crystalloid body is often observed at the posterior end (green fluorescence), but can also be observed in the mid-region of the sporozoite where it wraps around the nucleus.

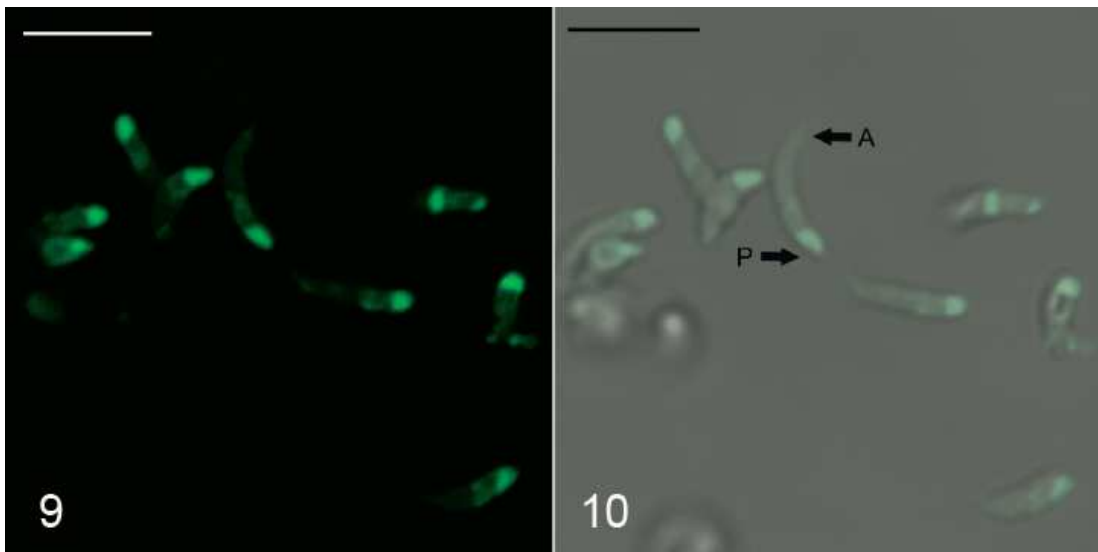
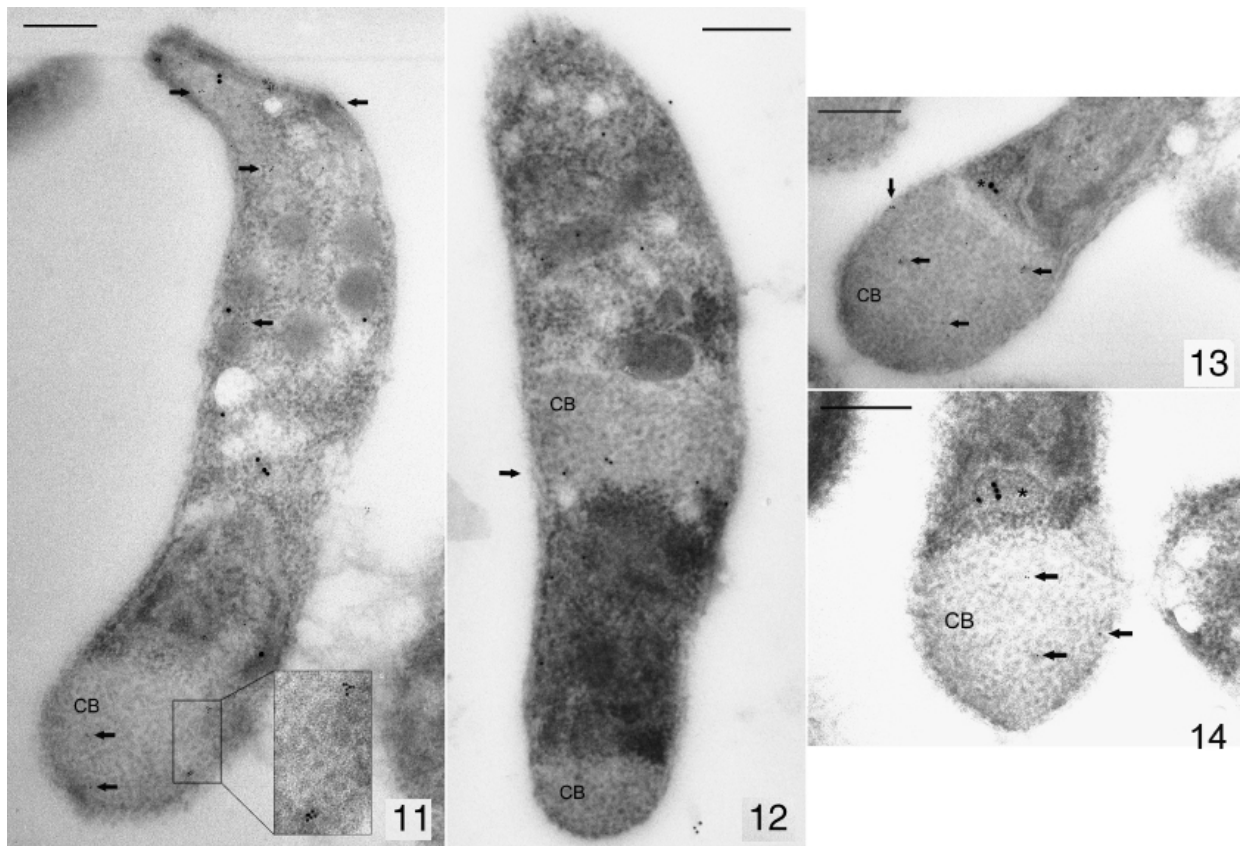


Figure 11 – 14. Transmission electron microscopy of *Cryptosporidium parvum* sporozoites showing immunogold localization of pyruvate:NADP⁺ oxidoreductase (CpPNO). Scale bars - 0.5 μ m. 11. Longitudinal section of sporozoite at high magnification showing the crystalloid body (CB), cytosol, and other organelles. The cytosol is double-labeled with control 15-nm gold anti-CpPPTase particles, and with 6-nm gold goat anti-CpPFO particles (arrows). The inset clearly shows clusters of 6-nm anti-CpPFO particles within the crystalloid body. 12. Single-labeling *C. parvum* sporozoites with 10-nm gold rabbit anti-CpPFO shows that both the cytosol and crystalloid body (arrow) are labeled. In this section, the CB can be seen to wrap around the nucleus. 13–14. Longitudinal section of the posterior end of the sporozoites. The mitochondrion (*) is posterior to nucleus, and lies between the nucleus and the CB. It is labeled by mitochondrion-specific 15-nm gold anti-CpCpn60 particles. Small, 6-nm gold goat anti-CpPFO particles (arrows) show the localization of CpPNO. There is no localization of 6-nm gold particles within the mitochondrion.



II A *Narf*-LIKE GENE FROM *Cryptosporidium parvum* RESEMBLES HOMOLOGUES OBSERVED IN AEROBIC PROTISTS AND HIGHER EUKARYOTES

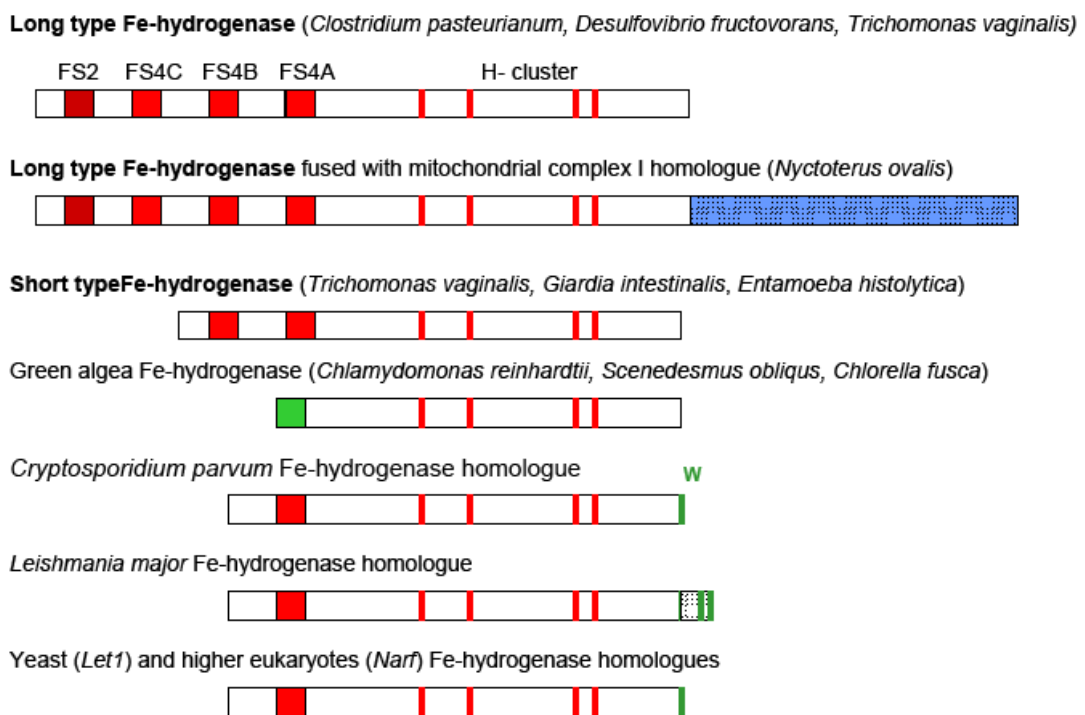
[Fe]-hydrogenases in hydrogenosomes

Formation of hydrogen is the key reaction, catalyzed by [Fe]-hydrogenases, which takes place in hydrogenosomes - organelles present in several types of anaerobic protists. In *Trichomonas*, pyruvate is oxidized by PFO and generated electrons are transferred to ferredoxin which, under anaerobic conditions, is reoxidized by Fe-hydrogenase that produces the molecular hydrogen (Muller, 1993). This process led to the naming of the hydrogenosome organelle (Lindmark and Muller, 1973). Hydrogenosomes are organelles that evolved independently in phylogenetically diverse groups of unicellular protists as they adapted to microaerophilic environment where they make energy and produce molecular hydrogen. They have been best studied in trichomonads, ciliates or chytrid fungi (Roger and Silberman, 2002). Hydrogenosomes are related to mitochondria with the same origin of endosymbiotic α -prokaryote (Embley *et al.*, 2003). Together with hydrogenosomes, other derivatives of mitochondria have been identified and described: mitochondrial remnants (mitosomes) in *Entamoeba histolytica* (Tovar *et al.*, 1999), microsporidian *Trachipleistophora hominis* (Williams *et al.*, 2002), *Giardia intestinalis* (Tovar *et al.*, 2003) and the relict mitochondrion in *C. parvum* (Slapeta and Keithly, 2004; Keithly *et al.*, 2005). Their common features include a double membrane containing a membrane potential, mitochondrial-type chaperones and the absence of Krebs cycle and respiratory chain enzymes. The possible reason that these highly reduced organelles have been retained, is probably for the separation of iron metabolism and the [FeS] cluster assembly, which may be toxic for the cell (LaGier *et al.*, 2003).

[Fe]-hydrogenases versus NARF-like proteins

[Fe]-hydrogenases are metabolically active metalloproteins containing an N-terminal [Fe-S] clusters and enzymatically active H clusters that forms the catalytic center of iron-only hydrogenases (Nicolet *et al.*, 2000). The presence of hydrogen producing [Fe]-hydrogenases is limited to anaerobic protozoa (trichomonads, entamoebas, diplomonads, ciliates), chytrid fungi, and green algae (Embley *et al.*, 2003). There may be one or more copies of [Fe]-hydrogenases in a genome. For example, *T. vaginalis* contains genes for three [Fe]-hydrogenases of different lengths and different content of [Fe-S] clusters that are targeted to hydrogenosome (Horner *et al.*, 2002) whereas *G. intestinalis* contains only one short [Fe]-hydrogenase localized in cytoplasm (Nixon *et al.*, 2003) (Fig. 15).

Figure 15. Prokaryotic and eukaryotic hydrogenase homologues.



Traces of [Fe]-hydrogenase genes can be found in each eukaryotic organism, even in our own genome and in all higher eukaryotes analyzed so far. However, these related genes code proteins lacking detectable hydrogenase activity. They are called **NARF-like proteins** according to the first [Fe]-hydrogenase-like gene discovered in humans (NARF protein; nuclear prelamin A recognition factor) (Barton and Worman, 1999), which function is well known. Human NARF is a nuclear protein that interacts with prenylated prelamin A, the precursor form of lamin involved in the maintenance of the structural integrity of the nucleus (Barton and Worman, 1999). The *Narf*-like genes show extensive similarity to the genes of [Fe]-hydrogenases, especially with respect to the conservation of residues in the unique active hydrogen cluster (H cluster) that is found in all [Fe]-hydrogenases. *Narf*-like genes are shorter than [Fe]-hydrogenase genes and some of them contain nuclear localization sequences. NARF-like proteins localization together with their absence of hydrogen production suggests that these proteins are probably not involved in energy metabolism (Horner *et al.*, 2000). Recently, it has been shown that yeast *Narf*-like protein (Nar1 protein) is involved in the cytoplasmic and nuclear [FeS] metabolism (Balk *et al.*, 2004).

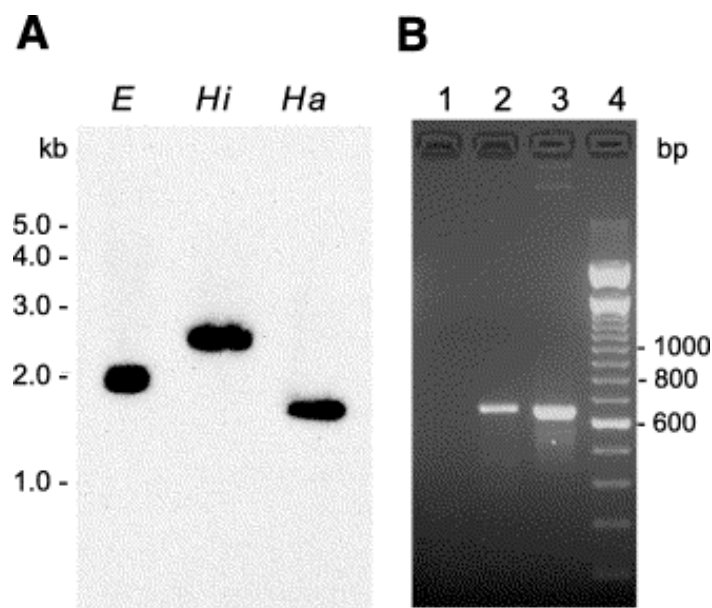
Even though [Fe]-hydrogenases or NARF-like proteins have been identified in all eukaryotes analyzed so far, no eukaryotic lineage that contains both a functional [Fe]-hydrogenase and a NARF-like protein have been found yet. It is unclear whether [Fe]-hydrogenases and NARF-like proteins share a common function or if they are both essential for eukaryotes. However, one experiment showed that the deletion of a *Narf*-like gene (*Nar1*) was lethal to haploid yeast cells, which indicates its importance in their overall metabolism and its necessity in at least one species (Winzeler *et al.*, 1999).

Results

In *C. parvum*, a [Fe]-hydrogenase-like fragment was identified (Stejskal *et al.*, 2003). The entire ORF was cloned into a pCR2.1 TOPO vector and sequenced. The nucleotide sequence of *CpNARF* gene was deposited to GenBank. The Southern blot analysis revealed that *CpNARF* is a single copy gene (Fig. 16). Its expression was

confirmed in both extracellular and intracellular stages of the parasite by RT-PCR (Fig. 16).

Figure 16. Southern blot and RT-PCR analysis of CpNARF. A: Southern blot analysis. 5 μ g of genomic DNA per lane was digested with *EcoRI* (E), *HindIII* (Hi) or *HaeIII* (Ha). The probe was an [α - 32 P]dATP random-primer-labeled DNA fragment of CpNARF (positions 534–1387). B: RT-PCR analysis. Lane 1: negative control (PCR without cDNA template); lane 2: PCR using gene-specific primers (cDNA from *C. parvum*-infected cells); lane 3: positive control (PCR with gene-specific plasmid DNA); lane 4: 100-bp ladder.



Multiple amino acid sequence alignment of [Fe]-hydrogenases with NARF-like proteins revealed a close relationship of *C. parvum* protein with NARF-like proteins from aerobic protists and higher eukaryotes instead of [Fe]-hydrogenases of microaerophilic protists and anaerobic bacteria (Fig. 17). This was confirmed by phylogenetic analysis of 37 taxa as it revealed that the gene from *C. parvum* clusters with the *Narf*-like genes from yeast, animals and higher plants and not with [Fe]-hydrogenases of anaerobic protist (*E. histolytica*, *G. intestinalis*, *T. vaginalis*, *Nyctotherus ovalis*) (Fig. 18). Thus, *C. parvum* gene has been classified as a *Narf*-like gene and was named *CpNARF*.

Figure 17. Multiple sequence alignment of conserved residues of [Fe]-hydrogenase homologues. *Trichomonas vaginalis* putative hydrogenosomal targeting sequence (dashed underline); *Homo sapiens* putative nucleus localization sequences (solid underline). FS4B and FS4A= two N-terminal accessory [4Fe-4S] binding clusters: * = conservative cysteines (C) within FS4B; + = conserved C within FS4A. Motifs 1–4 belong to the H-cluster: ↓ = conserved C within H-cluster; ● = polar and ○ = hydrophobic amino acid residues of the H-cluster active site determined from the crystal structure of *Clostridium pasteurianum* [Fe]-hydrogenase. Abbreviations: Cl.p, *Clostridium pasteurianum*; T.v.A, *Trichomonas vaginalis* hydA3; E.hi, *Entamoeba histolytica*; G.in, *Giardia intestinalis*; Ch.r, *Chlamydomonas reinhardtii* hydA; C.pa, *Cryptosporidium parvum*; L.ma, *Leishmania major*; S.ce, *Saccharomyces cerevisiae* Nar1; E.cu, *Encephalitozoon cuniculi*; H.sa, *Homo sapiens* Narf (#AAD51446); A.th, *Arabidopsis thaliana*; T.go, *Toxoplasma gondii*, incomplete Narf-like ORF: gln/TIGR 5811/contig:5468:t gondii. Note: Ch.r does not contain the N-terminal FS4B and FS4A clusters; T.go partial ORF contains a sequence homologous to [Fe]-hydrogenase motifs 2, 3 and 4 within the H-cluster.

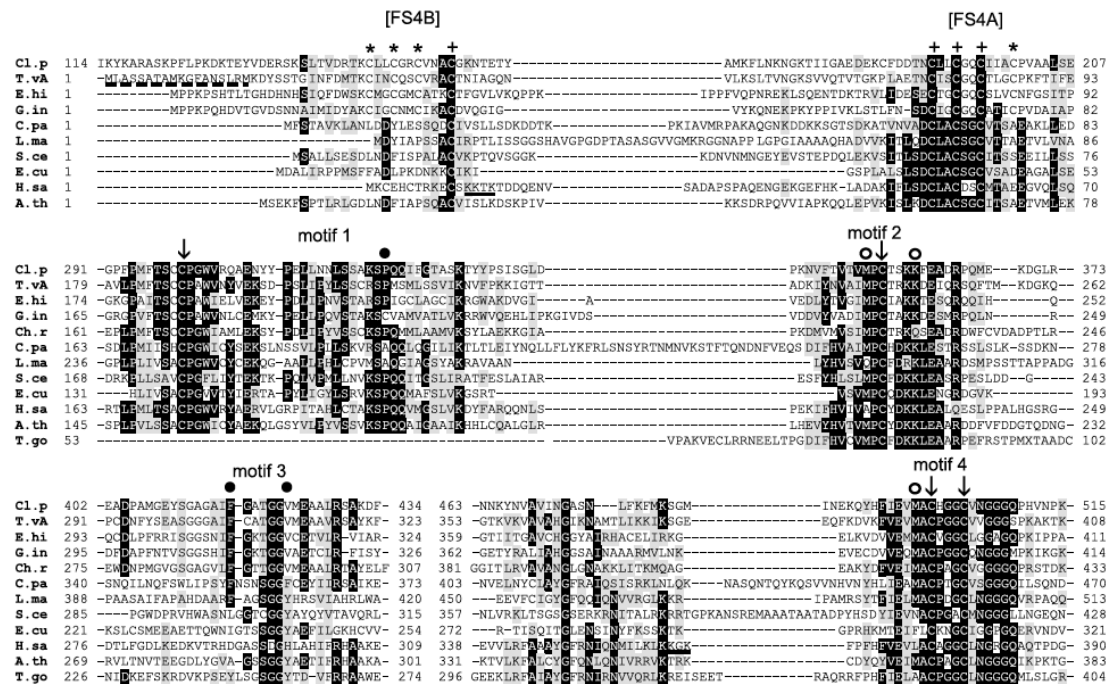
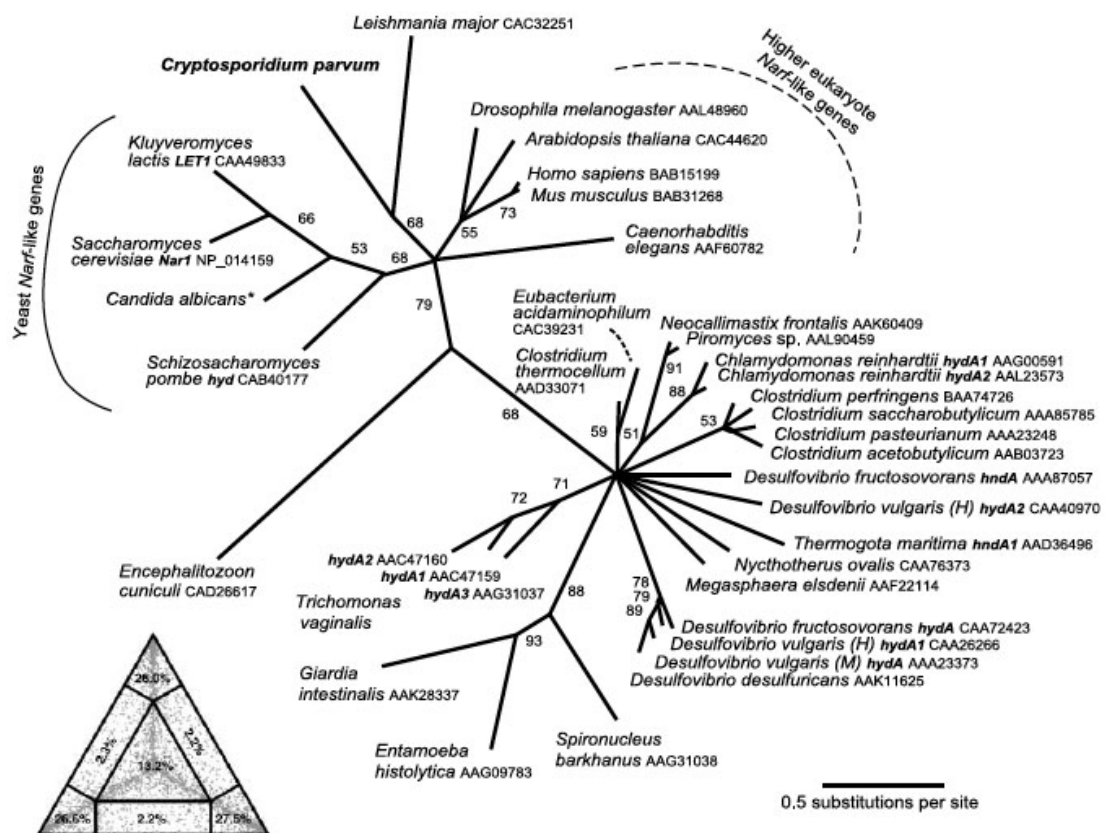


Figure 18. The phylogenetic relationship among major [Fe]-hydrogenase clusters is based upon amino acids conceptually translated from recovered DNA sequences of 37 taxa. The phylogram was reconstructed in TREE-PUZZLE based on [Fe]-hydrogenase and *NARF*-like amino acid sequence alignments using the WAG + Γ + θ model of amino acid evolution (log - Ln = - 15 912). The numbers at the internal branches represent the quartet puzzling values (n=1000). The inset diagram represents a likelihood mapping analysis of [Fe]-hydrogenase sequence alignments. The regions at the three corners of the triangle represent well-resolved phylogeny. The central region represents star-like evolution. The three sides of the triangle represent regions where it was difficult to distinguish between two of three topologies with an equal likelihood, and in which the third topology had a probability of zero. **Candida albicans* full length *Narf*-like ORF: gln/SDSTC_5476/C.albicans Contig6-2352.



To summarize the obtained data; in *C. parvum*, i) the residues of H-cluster (composed of [4Fe-4S] and [2Fe] clusters) and FS4A domain (an adjacent medial Fe-S cluster) were identified; ii) neither electron accepting domain nor organellar targeting signal or nuclear localization sequences were detected; iii) a putative proton donating C conserved in hydrogen producing hydrogenases was not found in *CpNARF*; iv) alike most of NARF like-proteins, *CpNARF* was found to contain a conserved tryptophan residue at the C-terminus; v) furthermore, [Fe]-hydrogenases enzymatic activity could not be detected in *C. parvum* sporozoite extract using standard assays (Hrdy and Stejskal, unpublished data). Although the function of this gene is as yet unknown, our phylogenetic analyses suggest that *CpNARF* belongs to the group of NARF-like proteins from aerobic protists and higher eukaryotes, which are thought to have had an ancestor in common with [Fe]-hydrogenases. [Fe]-hydrogenases appear to have diverged in both structure and function as core metabolism changed in aerobic and anaerobic eukaryotic lineages over evolutionary time.

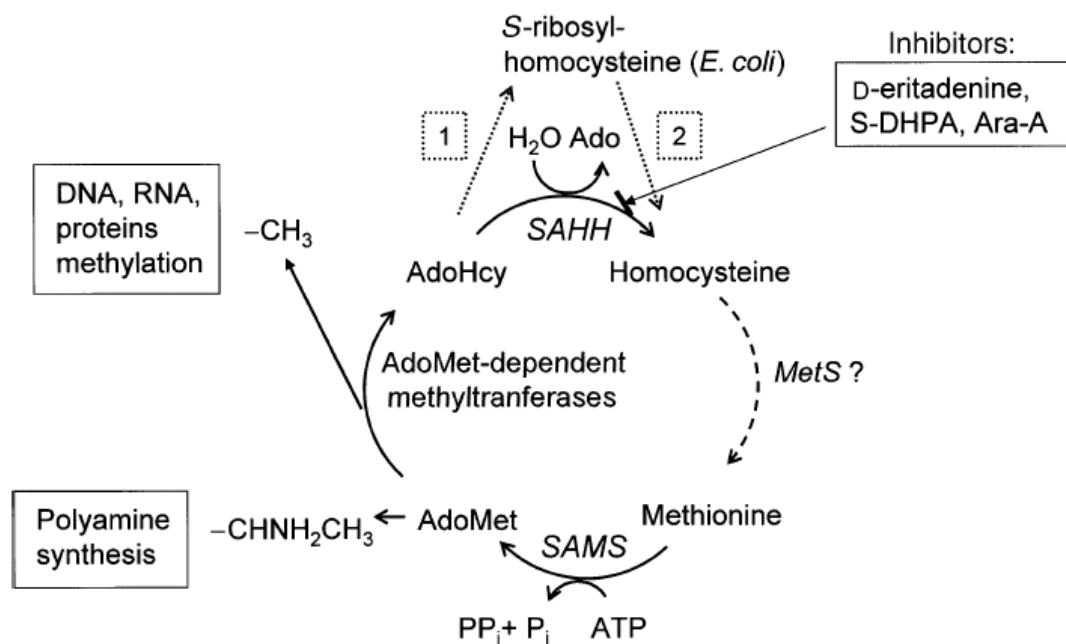
III CHARACTERIZATION OF S-ADENOSYLHOMOCYSTEINE HYDROLASE FROM *Cryptosporidium parvum*

S-adenosylmethionine metabolic pathway

Amino acids containing sulphur: methionine and cysteine, are a part of virtually every protein. Despite sulphur amino acids general utility, sulfur itself is toxic and its handling needs to be carefully regulated. Its regulation includes transsulfuration, sulfur assimilatory *de novo* cysteine biosynthesis, methionine cycle and degradation which involve at least two dozen intermediates and products. If these sulphur containing amino acids and some of their intermediates are not completely metabolized, their accumulation can have a very dangerous and even fatal impact to the overall metabolism. Although these two amino acids are indispensable for all living organisms, there are remarkable differences in their biosynthesis and catabolism between parasitic protozoa and their mammalian hosts (Nozaki *et al.*, 2005). Our understanding of these differences is crucial as it can help us to identify and exploit unique targets to develop novel chemotherapeutic and prophylactic agents.

One of the important sulphur-containing intermediates is S-adenosylhomocysteine. This compound is catabolized by the enzyme S-adenosylhomocysteine hydrolase (SAHH) into adenosine and L-homocysteine (De La Haba and Cantoni, 1959). If SAHH is inhibited, S-adenosylhomocysteine accumulates in the cytoplasm where it acts as a potent feedback inhibitor and blocks methylation reactions by inhibiting S-adenosylmethionine-dependent methyltransferases, thus influencing the overall methylation capacity of the cell (Fig. 19) (Turner *et al.*, 2000).

Figure 19. S-adenosylmethionine metabolic pathway. The abbreviations are: S-adenosylmethionine (AdoMet), S-adenosylhomocysteine (AdoHcy), S-adenosylhomocysteine hydrolase (SAHH), methionine synthetase (MetS): no orthologs of this enzyme have yet been found in *Cryptosporidium parvum* (Abrahamsen *et al.*, 2004; Thompson *et al.*, 2005), S-adenosylmethionine synthetase (SAMS). The S-adenosylhomocysteine degradation pathway in *Escherichia coli* is indicated with dashed lines. Enzymes in this pathway are (1) S-adenosylhomocysteine nucleosidase, (2) S-ribosylhomocysteinase.



SAHH from different organisms

SAHH has been isolated from many organisms including humans (Hershfield *et al.*, 1985), rats (Fujioka and Takata, 1981), plants (Guranowski and Pawelkiewicz, 1977; Sebestova *et al.*, 1984), yeast (Knudsen and Yall, 1972), protozoa: *Trichomonas vaginalis* (Bagnara *et al.*, 1996), *Plasmodium falciparum* (Creedon *et al.*, 1994), prokaryotes (Porcelli *et al.*, 1993; Porcelli *et al.*, 2005) and characterized. Several of these SAHH have been examined, their biochemical properties and enzymatic activities have been measured (Creedon *et al.*, 1994; Minotto *et al.*, 1998; Porcelli *et al.*, 2000) and several crystal structures of SAHH have been elucidated: e.g. human (Yang *et al.*, 2003), rat (Hu *et al.*, 1999; Huang *et al.*, 2002), and *Plasmodium*

falciparum (Tanaka *et al.*, 2004). However, not all organisms contain this enzyme. For example, *Escherichia coli* dispenses with SAHH (Shimizu *et al.*, 1984), and because of its absence this bacterium is exploited as a background free organism for cloning.

For instance, SAHH from *P. falciparum* has been studied extensively as a potential drug target against malaria for a long time. Nevertheless, it has not been proposed to use this enzyme as a target protein for treatment against *Cryptosporidium*. Here, we characterized CpSAHH and showed that this protein is also suitable as a drug target against *C. parvum*.

Results

In drug development against any parasite it is essential to select targets from pathways that are present in the parasite but absent from humans. In the case of SAHH, this potential target is common in both the parasite and the host. Nevertheless, even if the target is common in parasite and host, slight structural difference such as single amino acid variation is likely to improve inhibitor selectivity. For instance, it has been shown that a single substitution of Cys⁵⁹ in *P. falciparum* and Thr⁶⁰ in humans accounted for the differential interactions with nucleoside inhibitors (Tanaka *et al.*, 2004). Furthermore, in contrast to human SAHH, CpSAHH contains a 49 aa long plant-like insertion (Fig. 20). Similar short amino acid insertions have been found in plants, a few eubacteria and some protists such as *P. falciparum*, *T. vaginalis* and *E. histolytica*. This insertion is absent in animals, fungi, kinetoplastids, Archaeobacteria and some Eubacteria. The exact function of this insertion is not known. However, the crystal structure of *P. falciparum* SAHH revealed that its plant like insertion is located at the edge of the substrate binding domain and might participate in the binding of a substrate (Tanaka *et al.*, 2004).

Figure 20. The partial alignment of CpSAHH and 12 other organisms. CpSAHH differs substantially from mammalian SAHH as it contains a 49 amino acid plant-like insertion.

		plant-like insertion sequence							
<i>C. parvum</i>	DGGDATLILH	EGVKAIEIYE	KYNKIPEYLE	TELDENGKQL	SMDLKCMYKV	LKMELLNPF	RWRGMLKDLY		
<i>P. falciparum</i>	DGGDATLLVH	KGVEYEKLYE	EKNILPDPEK	AK.....	NEEERCFLTL	LKNSILKNPK	KWTNIAKKII		
<i>C. roseus</i>	DGGDATLLIH	EGVKAEEYK	KNGALPDPSS	TD.....	NAEFQIVLTI	IRDGLKSDPT	KYTRMKERLV		
<i>T. vaginalis</i>	DGGDATLLIS	KGFEFE....	TAGAVPEPTE	AD.....	NLEYRCVLAT	LKQVFNQDKN	HWHTVAAGMN		
<i>E. histolytica</i>	DEGDATLMIH	TGYHAEExxx	KNIQEILDVK	G.....	TEEVNALHNV	LKKQLKENPR	FWHNILPEIR		
<i>M. tuberculosis</i>	DGGDATMLVL	RGMQ....YE	KAGVPPAEE	DDP.....	.AEWKVFLNL	LRTRFETDKD	KWTKIAESVK		
<i>H. sapiens</i>	DGGDLTNLIHT	KYPQLLPGIF	
<i>D. melanogaster</i>	DGGDLTNLVH	E.....	KFPQFLKNIF	
<i>S. cerevisiae</i>	DGGDLTTLVH	E.....	KHPEMLEDCF	
<i>P. carinii</i>	DGGDVTSLVHN	KYPDYLKNCF	
<i>L. donovani</i>	DGGDLTNLVI	D.....	HHPELVPKIF	
<i>Synechocystis</i>	DGSDVVATLV	Q.....	ERQHQLSDII	
<i>P. horikoshii</i>	DGADMISLVH	K.....	ERQELLEIV	

Using Southern blot analysis, it was revealed that CpSAHH is present in the genome as a single copy gene which was later confirmed by whole genome sequencing (Abrahamsen *et al.*, 2004). The CpSAHH expression profile was determined with RT-PCR analysis (Fig. 21) which showed that the *CpSAHH* gene was expressed both in sporozoites and in the intracellular stages multiplying in HCT-8 cells. Multiple sequence analysis of CpSAHH and other selected prokaryotic and eukaryotic SAHH homologues indicated that CpSAHH contains most of the amino acid residues and motifs necessary for enzymatic activities. The complete *CpSAHH* gene was cloned into the pMAL-c2X vector and was expressed in *E. coli* TB1 cells as an MBP-fusion protein. After purification, the cleaved denatured protein was subjected to SDS-PAGE to establish its subunit molecular mass (Fig. 22) and the recombinant native protein was subjected to the size-exclusion chromatography on a Superdex 200 column. The apparent molecular mass of the native protein is about 244-kDa. This suggested that *CpSAHH* is a tetramer which is in agreement with SAHH proteins in variety of organisms (Fujioka and Takata, 1981; Porcelli *et al.*, 1993; Tanaka *et al.*, 2004).

Figure 21. RT-PCR analysis of *CpSAHH* expression in *Cryptosporidium parvum* sporozoites (lanes 2, 3) and *C. parvum* intracellular stages in HCT-8 cells (lanes 4–7). The presence of RNA and reverse transcriptase (RTase) are indicated. Lane 1, negative control – reaction without RNA; lanes 2 and 3, expression in sporozoites; lanes 4 and 5, RNA isolated from uninfected HCT-8 cells; lanes 6 and 7, RNA isolated from 24 h *C. parvum* – infected HCT-8 cells; lane 8, positive control – *CpSAHH* DNA.

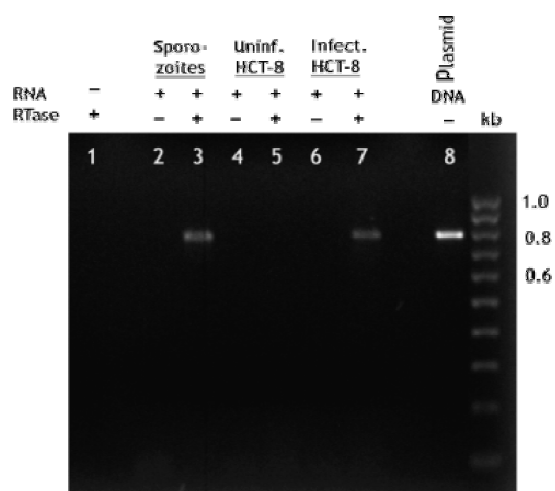
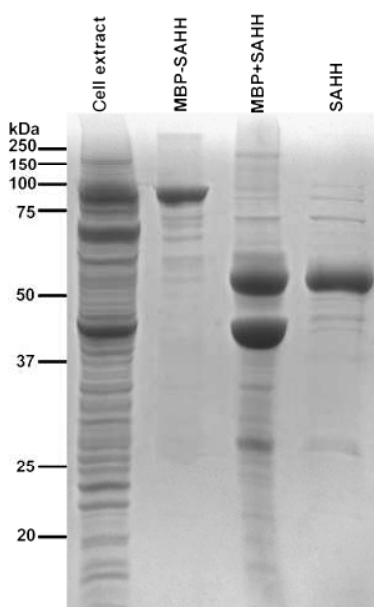


Figure 22. SDS-PAGE analysis of the purification of the recombinant SAHH. The molecular mass standard is a Precision Plus protein standard (Bio-Rad). Lane 1, crude cell lysate before its application to the amylose column; lane 2, affinity purified fusion protein MBP-CpSAHH; lane 3, cleaved fusion protein by Factor Xa; lane 4, CpSAHH eluted from a hydroxyapatite column.



As was predicted from amino acid sequence comparisons, CpSAHH retained its enzymatic activity. Its activity was tested spectrophotometrically in the hydrolytic direction. The enzyme kinetic profiles (K_m , K_{cat} , V_{max}) of both CpSAHH and MBP-CpSAHH were determined (Fig. 23). Results showed that the kinetic profiles of CpSAHH and MBP-CpSAHH differed as the MBP tag seemed to slow down the enzymatic reaction. However, in comparison to known kinetic profiles from other organisms, CpSAHH falls within their range (Table 2). The catalytic turnover of CpSAHH was determined to be $K_{cat} = 0.69 \text{ s}^{-1}$ which falls in the range of known values $K_{cat} = 0.13 - 3.8 \text{ s}^{-1}$ (Fujioka and Takata, 1981; Yuan *et al.*, 1996; Porcelli *et al.*, 2000).

Figure 23. Michaelis–Menten kinetics of MBP-CpSAHH (○) and CpSAHH (●) displayed in a Lineweaver–Burk plot for determination of V_{max} and K_m . S-adenosylhomocysteine was used as a substrate.

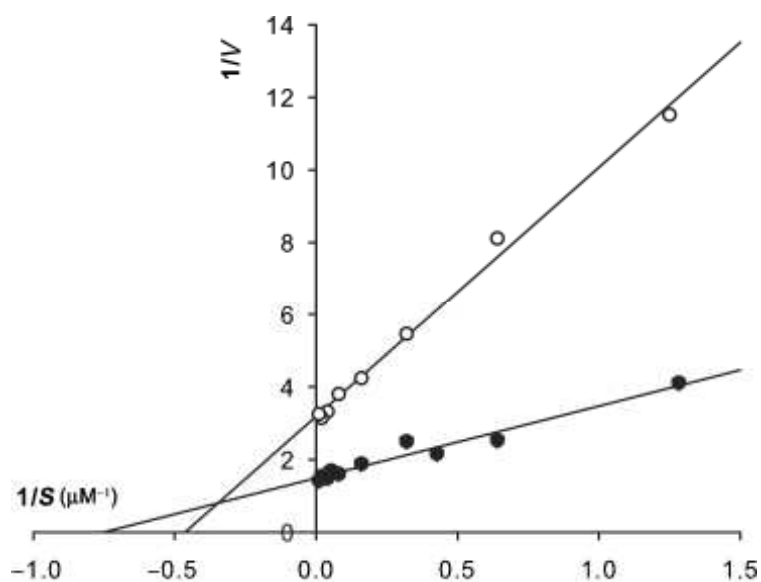


Table 2. Comparison of *Cryptosporidium parvum* SAHH activity with SAHH activities from other organisms measured in the hydrolytic direction.

Source	K_m (μM)	V_{\max} ($\mu\text{M}\cdot\text{min}\cdot\text{mg}^{-1}$)	K_{cat} (s^{-1})
<i>C. parvum</i> SAHH	1.31 ± 0.20	0.74 ± 0.07	0.69
<i>C. parvum</i> MBP-SAHH	2.69 ± 0.11	0.29 ± 0.05	0.46
<i>L. donovani</i> SAHH	21.00 ± 3.00	0.17	0.48
<i>P. falciparum</i> SAHH	1.2 ± 0.10	-	0.02
<i>R. rattus</i> SAHH	15.20 ± 1.11	1.08 ± 0.03	0.85
<i>H. sapiens</i> SAHH	7.80 ± 0.20	-	0.53
<i>S. solfataricus</i> SAHH	14.00	0.17	0.13

In a pilot experiment, it was found that three compounds Ara-A, S-DHPA and EritA were able to inhibit CpSAHH at low concentrations (Table 3). One of these inhibitors is the cyclic compound: **Ara-A**. This drug has been approved and primarily used as an antiviral agent that displays a wide antiviral spectrum. Inhibition of SAHH by Ara-A has been studied in detail. Ara-A targets the active site of the enzyme, and causes the irreversible inactivation of isolated or recombinant SAHH and reduces the enzyme bound NAD^+ (Helland and Ueland, 1982). It seems that Ara-A can be directed to a number of targets. In agreement with inhibition of recombinant SAHH from *T. vaginalis* (Minotto *et al.*, 1998), 500 nM Ara-A inhibited CpSAHH by 17.5% (Table 3). The other two inhibitors used are adenosine analogues with acyclic sugar moieties and both of them are known potent antiviral agents (Holy *et al.*, 1985). Neither of them has been tested against SAHH from parasitic protozoa. **S-DHPA** displayed similar inhibition as Ara-A. At a concentration of 500 nM, the enzymatic activity of CpSAHH remained at the 86% of the control, so S-DHPA inhibited CpSAHH by 14% (Table 3). However, **D-eritadenine** (EritA) proved to be very efficient inhibitor of CpSAHH. 500 nM EritA inhibited CpSAHH activity by 95.3%, the remaining enzymatic activity was 4.7% (Table 3). EritA seemed to be a very promising drug especially in the light of the previous success as an efficient antiviral agent. In the experiments with EritA and vaccinia virus, vesicular stomatitis virus or measles virus in primary rabbit kidney cells, EritA proved to be rather selective. Inhibition of the replication of viruses occurred in concentrations of 10 - 100 $\mu\text{g}/\text{ml}$, whereas host cell cytotoxicity was not observed until 400 $\mu\text{g}/\text{ml}$ (De

Clercq *et al.*, 1984).

Table 3. Effect of nucleoside analogues on the activity of recombinant CpSAHH.

Inhibitors	Concentration (nM)	Enzyme activity (% of control)
Control	0	100
D-eritadenine	10	91.58
	100	69.34
	500	4.74
	1000	5.18
S-DHPA	10	97.32
	100	93.31
	500	86.09
	1000	66.91
Ara-A	10	100
	100	90.36
	500	83.51
	1000	73.30

Unpublished results

Even though there has been shown a certain level of inhibition of the recombinant CpSAHH by aliphatic adenosine analogues in the pilot experiment, inhibition of CpSAHH needed to be further tested in the microenvironment of the host cell and in the context of the whole organism. That is why; the inhibition of CpSAHH has been tested under *in vitro* conditions.

The measurements of SAHH inactivation, in parasites that infected human HCT-8 cells, were based on quantitative real-time reverse transcription-PCR (qRT-PCR). The relative expression was determined by detection of both host cell 18S rRNA ($C_{T[H18S]}$) as an internal control and parasite 18S rRNA ($C_{T[P18S]}$). The level of parasite 18S rRNA was subsequently calculated as a ratio of C_T values ($\Delta C_T = C_{T[P18S]} - C_{T[H18S]}$). The data was further processed and statistically analyzed (Cai *et al.*, 2005). We employed qRT-PCR assay to evaluate the efficiency of used aliphatic inhibitors, which were previously shown to have also antiviral activity (Holy *et al.*,

1985), on the growth of *C. parvum in vitro*. All used inhibitors displayed a dose-dependent inhibition of the intracellular stages of *C. parvum* cultured with HCT-8 cells (Fig. 24- 26). The IC_{50} was determined by nonlinear curve regression. The IC_{50} values for (S)-DHPA, (R)-DHPA and EritA were determined to be 4.3 μ M, 11.6 μ M and 44.8 μ M, respectively. No significant cytotoxicity to HCT-8 cells was observed at used concentrations by the MTT assay (a standard colorimetric assay for measuring cellular growth and cytotoxicity of potential medicinal agents).

Figure 24. Efficacy of (S)-DHPA on the growth of *C. parvum in vitro*, as determined by qRT-PCR.

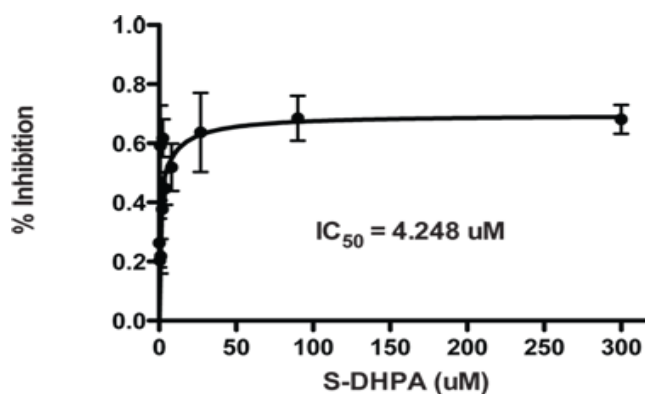


Figure 25. Efficacy of (R)-DHPA on the growth of *C. parvum in vitro*, as determined by qRT-PCR.

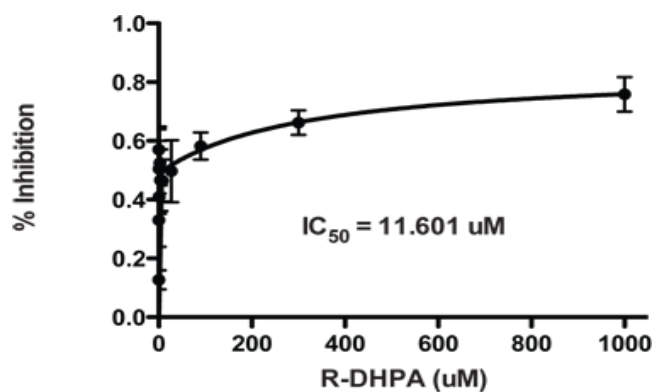
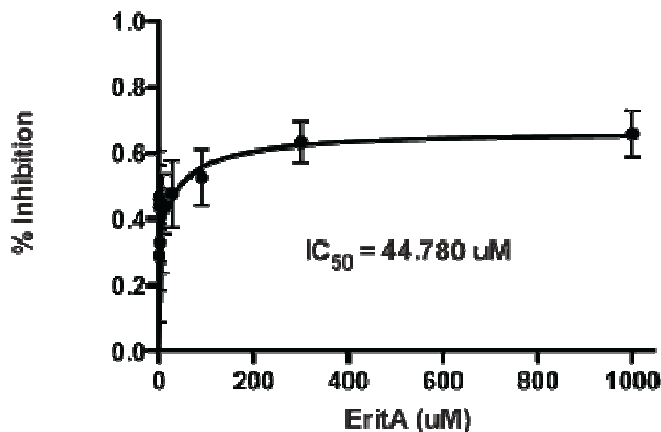


Figure 26. Efficacy of EritA on the growth of *C. parvum in vitro*, as determined by qRT-PCR.



The drug efficiencies were compared with two golden standards used in drug testing against *C. parvum*: paromomycin, a compound that inhibits protein synthesis by binding to 18S rRNA (Marshall and Flanigan, 1992) and nitazoxanide, a drug, which is approved for the treatment of infectious diarrhea caused by *C. parvum* and *G. intestinalis* in patients 1 year of age and older in USA (Bailey and Erramouspe, 2004). After comparison, the data showed that inhibition of the growth of *C. parvum in vitro* with (S)-DHPA, (R)-DHPA and EritA, respectively, was more potent than when using paromomycin ($IC_{50} = 137 \mu M$) (Cai *et al.*, 2005). The potential to inhibit intracellular stages of *C. parvum* was also elucidated with NTZ from other study ($IC_{50} = 0.98 \mu M$) (Cai *et al.*, 2005). The inhibition of CpSAHH using (S)-DHPA was efficient enough even though it did not reach the level of NTZ. Nevertheless, it can be claimed that (S)-DHPA and (R)-DHPA may be explored as potential drug targets for the control of *C. parvum* infection. Interestingly, the most potent inhibitor of the recombinant protein, EritA was the least potent inhibitor of the CpSAHH in *in vitro* experiment. This results is in agreement with previous studies (Holy *et al.*, 1985) describing that particular inhibitors can be very potent against isolated and recombinant proteins but to have only minimal effect on SAHH catabolism in intact cells or vice versa. For example, (S)-DHPA caused no inactivation of isolated SAHH

from rat hepatocytes although it proved efficient as an inhibitor in intact liver cells (Schanche *et al.*, 1984) This effect could have been caused by the uptake of (S)-DHPA, the inhibitor might have been modified in the microenvironment of the cell and become more toxic. On the other hand, some inhibitors such as 2-chloroadenosine proved to be extremely efficient in inhibiting the isolated enzyme but not very efficient in intact lymphocytes (Zimmerman *et al.*, 1980). This suggests that if these inhibitors actually penetrate an organism then they get rapidly metabolized. Furthermore, SAHH from different organisms responds differently to the same inhibitor because their amino acid composition is not usually completely congruent. All these unpredictable factors make designing of potential drugs difficult and each inhibitor must be carefully tested in all conditions. Further studies are needed to assess whether these adenosine analogues could be developed into new anticryptosporidial drugs.

SUMMARY.

Cryptosporidium parvum is a unicellular parasite that belongs to the Phylum Apicomplexa. This parasite can infect both humans and animals, causing an acute diarrhea in immunocompetent individuals, and a chronic life threatening infection in immunocompromised persons. *Cryptosporidium* is a problematic species that almost does not respond to commonly used drugs against its related parasites (e.g. Coccidia) because in contrast to other parasites, *C. parvum* metabolism has been streamlined to include only components of vital concern. The parasite has lost or diverted many enzymes and metabolic pathways present in other apicomplexans. Thus, *C. parvum* does not possess many well-studied potential drug targets (e.g. HXGPRT, ODC, mannitol cycle, shikimate pathway, Krebs cycle and an entire apicoplast). However, the parasite does encode several other potential drug targets, some of which are unique, gained by horizontal transfer from another organism such as plants or bacteria. Additionally, it possesses some aspects that have been likely gained through endosymbiosis and contains proteins that are highly divergent or absent in humans and animals (Huang *et al.*, 2004).

Even though our general understanding of the *C. parvum* metabolic machinery have significantly increased by now, our knowledge of many specific pathways and enzymes in *Cryptosporidium* is still limited. A better understanding of important metabolic pathways and enzymes in this organism would aid in the experimentation of new drugs and developing new strategies to treat this infection in humans and animals.

Via the fulfillments of given research objectives in this dissertation the results presented bring a characterization of three potential drug targets from *C. parvum*: pyruvate:NADP⁺ oxidoreductase, S-adenosylhomocysteine hydrolase and a *CpNARF*:

Pyruvate:NADP⁺ oxidoreductase

- In contrast to PNO in *Euglena gracilis*, CpPNO is a cytosolic, not mitochondrial protein, which was confirmed by both confocal immunofluorescence and immunogold labeling for TEM. This new data is in agreement with the suggestion that the relict mitochondrion of *C. parvum* serves primarily as an organelle for the import and maturation of Fe-S clusters and that it plays no major role in core energy metabolism.
- Both confocal images and immunogold labeling showed that CpPNO is localized also within the crystalloid body, as well as within the cytosol. These data, together with the close juxtaposition of the CB and the relict mitochondrion, as well as their distinctive internal structure, indicate that there may be some interesting evolutionary implications for why the CB remains a unique subcompartment within *C. parvum*. Because CpPNO is compartmentalized in a novel way, it opens the possibility that this apicomplexan may display yet another unique type of core energy metabolism in microaerophilic protists that might lead to new strategies for drug development against human cryptosporidiosis.
- The uptake and localization of fluorescent dyes (Mitotracker Green FM, Rhodamine B and Rhodamine 123) into both the CB and the relict mitochondrion was shown, which might indicate an organellar membrane potential in spite of neither TEM nor tomographic reconstruction could resolve whether the CB is membrane bounded.

***CpNARF* gene**

- In *C. parvum*, an [Fe]-hydrogenase-like gene had been identified and characterized. This gene contains a single highly conserved N-terminal iron-sulfur cluster ([4Fe-4S]) binding site, as well as most of the H-cluster conserved residues and lacks the obvious N-terminal organelle-targeting signal, present in most metabolically active [Fe]-hydrogenases.
- RT-PCR analysis revealed that *CpNARF* gene is expressed by the intracellular stages of *C. parvum* and it encodes putative protein of 560 amino acids, which was named CpNARF.
- Phylogenetic analysis revealed that the *CpNARF* gene from *C. parvum* clustered with the *Narf*-like genes from yeast, animals and higher plants. *CpNARF* gene did not cluster with [Fe]-hydrogenases of anaerobic protists (*E. histolytica*, *G. intestinalis*, *S. barkhanus*, *T. vaginalis*, *Nyctotherus ovalis*).
- Although the function of this gene is unknown, both phylogenetic analyses and sequence data suggest that CpNARF belongs to the group of NARF-like proteins from aerobic protists and higher eukaryotes, which are thought to have had an ancestor in common with [Fe]-hydrogenases.

S-adenosylhomocysteine hydrolase

- CpSAHH has been cloned and analyzed. The protein differs substantially from mammalian SAHH homologues and other nonapicomplexan protists as it contains a 49 amino acid plant-like insertion.
- CpSAHH is expressed both in intracellular stages (in *C. parvum*-infected HCT-8 cells) and in sporozoites.
- CpSAHH was expressed as a fusion protein MBP-CpSAHH, cleaved and purified. Enzymatic activities of both MBP-CpSAHH and CpSAHH (K_m , V_{max} , K_{cat}) were determined using the Michaelis-Menten plot. When compared to known kinetic profiles of SAHH from other organisms, CpSAHH falls within their range.
- Tertiary structure of the recombinant CpSAHH is a tetramer like most of the studied SAHH proteins.
- The enzymatic activity of CpSAHH was inhibited by D-eritadenine, (S)-DHPA and Ara-A. The most efficient inhibitor of the recombinant CpSAHH was D-eritadenine; 500 nM D-eritadenine inhibited CpSAHH activity by 95.3%
- Inhibitors (S)-DHPA, (R)-DHPA and D-eritadenine were observed to inhibit *C. parvum* growth *in vitro*, in infected human HCT-8 cells. The IC_{50} values for S-DHPA, R-DHPA and D-eritadenine were 4.3 μ M, 11.6 μ M and 44.8 μ M, respectively. Based on results presented in this dissertation both (S)-DHPA and (R)-DHPA were proven to be good candidates for next step in drug development against cryptosporidiosis.

REFERENCES

- Abrahamsen MS, Templeton TJ, Enomoto S, *et al.* Complete genome sequence of the apicomplexan, *Cryptosporidium parvum*. *Science* 2004; **304** (5669):441-5.
- Adjei A, Lartey M, Adiku TK, *et al.* *Cryptosporidium* oocysts in Ghanaian AIDS patients with diarrhoea. *East Afr Med J* 2003; **80** (7):369-72.
- Amadi B, Mwiya M, Musuku J, *et al.* Effect of nitazoxanide on morbidity and mortality in Zambian children with cryptosporidiosis: a randomised controlled trial. *Lancet* 2002; **360** (9343):1375-80.
- Anguish LJ, Ghiorse WC. Computer-assisted laser scanning and video microscopy for analysis of *Cryptosporidium parvum* oocysts in soil, sediment, and feces. *Applied and Environmental Microbiology* 1997; **63** (2):724-33.
- Bacchi CJ, Yarlett N. Polyamine metabolism as chemotherapeutic target in protozoan parasites. *Mini Rev Med Chem* 2002; **2** (6):553-63.
- Bagnara AS, Tucker VE, Minotto L, *et al.* Molecular characterisation of adenosylhomocysteinase from *Trichomonas vaginalis*. *Mol Biochem Parasitol* 1996; **81** (1):1-11.
- Bailey JM, Erramouspe J. Nitazoxanide treatment for giardiasis and cryptosporidiosis in children. *Ann Pharmacother.* 2004 Apr;**38**(4):634-40.
- Balk J, Pierik AJ, Netz DJ, Mühlenhoff U, Lill R. The hydrogenase-like Nar1p is essential for maturation of cytosolic and nuclear iron-sulphur proteins. *EMBO J.* 2004 May 19;**23**(10):2105-15.
- Barton RM, Worman HJ. Prenylated prelamin A interacts with Narf, a novel nuclear protein. *J Biol Chem* 1999; **274** (42):30008-18.
- Blackman MJ, Bannister LH. Apical organelles of Apicomplexa: biology and isolation by subcellular fractionation. *Mol Biochem Parasitol* 2001; **117** (1):11-25.

- Boxma B, de Graaf RM, van der Staay GW, van Alen TA, Ricard G, Gabaldón T, van Hoek AH, Moon-van der Staay SY, Koopman WJ, van Hellemond JJ, Tielens AG, Friedrich T, Veenhuis M, Huynen MA, Hackstein JH. An anaerobic mitochondrion that produces hydrogen. *Nature*. 2005 Mar 3;**434**(7029):74-9.
- Caccio SM, Thompson RC, McLauchlin J, Smith HV. Unravelling *Cryptosporidium* and *Giardia* epidemiology. *Trends Parasitol* 2005; **21** (9):430-7.
- Cai X, Lancto CA, Abrahamsen MS, Zhu G. Intron-containing beta-tubulin transcripts in *Cryptosporidium parvum* cultured in vitro. *Microbiology*. 2004 May;**150**(Pt 5):1191-5.
- Cai X, Woods KM, Upton SJ, Zhu G. Application of quantitative real-time reverse transcription-PCR in assessing drug efficacy against the intracellular pathogen *Cryptosporidium parvum* in vitro. *Antimicrob Agents Chemother*. 2005 Nov;**49**(11):4437-42.
- Carey CM, Lee H, Trevors JT. Biology, persistence and detection of *Cryptosporidium parvum* and *Cryptosporidium hominis* oocyst. *Water Res* 2004; **38** (4):818-62.
- Carmena D, Aguinagalde X, Zigorraga C, Fernandez-Crespo JC, Ocio JA. Presence of *Giardia* cysts and *Cryptosporidium* oocysts in drinking water supplies in northern Spain. *J Appl Microbiol* 2007; **102** (3):619-29.
- Chacin-Bonilla L. [*Cryptosporidium*: phylogeny and taxonomy]. *Invest Clin* 2007; **48** (1):1-4.
- Chappell CL, Okhuysen PC, Langer-Curry R, *et al.* *Cryptosporidium hominis*: experimental challenge of healthy adults. *Am J Trop Med Hyg* 2006; **75** (5):851-7.
- CDC: Preventing Cryptosporidiosis: A Guide to Water Filters and Bottled Water. http://www.cdc.gov/ncidod/dpd/parasites/cryptosporidiosis/factsht_crypto_event_water.htm.
- Chen XM, Keithly JS, Paya CV, LaRusso NF. Cryptosporidiosis. *N Engl J Med* 2002; **346** (22):1723-31.

- Chen XM, O'Hara SP, Huang BQ, *et al.* Apical organelle discharge by *Cryptosporidium parvum* is temperature, cytoskeleton, and intracellular calcium dependent and required for host cell invasion. *Infect Immun* 2004; **72** (12):6806-16.
- Chmelik V, Ditrich O, Trnovcova R, Gutvirth J. Clinical features of diarrhoea in children caused by *Cryptosporidium parvum*. *Folia Parasitol (Praha)* 1998; **45** (2):170-2.
- Clark DP. New insights into human cryptosporidiosis. *Clin Microbiol Rev* 1999; **12** (4):554-63.
- Colford JM, Jr., Tager IB, Hirozawa AM, *et al.* Cryptosporidiosis among patients infected with human immunodeficiency virus. Factors related to symptomatic infection and survival. *Am J Epidemiol* 1996; **144** (9):807-16.
- Coombs GH, Muller S. Recent advances in the search for new anti-coccidial drugs. *Int J Parasitol* 2002; **32** (5):497-508.
- Craik SA, Weldon D, Finch GR, Bolton JR, Belosevic M. Inactivation of *Cryptosporidium parvum* oocysts using medium- and low-pressure ultraviolet radiation. *Water Res* 2001; **35** (6):1387-98.
- Creedon KA, Rathod PK, Wellems TE. *Plasmodium falciparum* S-adenosylhomocysteine hydrolase. cDNA identification, predicted protein sequence, and expression in *Escherichia coli*. *J Biol Chem* 1994; **269** (23):16364-70.
- Ctrnacta V, Ault JG, Stejskal F, Keithly JS. Localization of pyruvate:NADP⁺ oxidoreductase in sporozoites of *Cryptosporidium parvum*. *J Eukaryot Microbiol* 2006; **53** (4):225-31.
- Ctrnacta V, Stejskal F, Keithly JS, Hrdy I. Characterization of S-adenosylhomocysteine hydrolase from *Cryptosporidium parvum*. *FEMS Microbiol Lett* 2007; **273** (1):87-95.
- Current WL, Garcia LS. Cryptosporidiosis. *Clin Microbiol Rev* 1991; **4** (3):325-58.
- Dan M, Wang CC. Role of alcohol dehydrogenase E (ADHE) in the energy metabolism of *Giardia lamblia*. *Mol Biochem Parasitol* 2000; **109** (1):25-36.

- Dann SM, Okhuysen PC, Salameh BM, DuPont HL, Chappell CL. Fecal antibodies to *Cryptosporidium parvum* in healthy volunteers. *Infect Immun* 2000; **68** (9):5068-74.
- De Clercq E, Bergstrom DE, Holy A, Montgomery JA. Broad-spectrum antiviral activity of adenosine analogues. *Antiviral Res* 1984; **4** (3):119-33.
- De La Haba G, Cantoni GL. The enzymatic synthesis of S-adenosyl-L-homocysteine from adenosine and homocysteine. *J Biol Chem* 1959; **234** (3):603-8.
- De Venevelles P., Francois CJ, Faigle W, *et al.* Study of proteins associated with the *Eimeria tenella* refractile body by a proteomic approach. *Int J Parasitol* 2006; **36** (13):1399-407.
- Deng M, Rutherford MS, Abrahamsen MS. Host intestinal epithelial response to *Cryptosporidium parvum*. *Adv Drug Deliv Rev* 2004;**56** (6):869-84.
- Deng MQ, Cliver DO. *Cryptosporidium parvum* studies with dairy products. *Int J Food Microbiol* 1999; **46** (2):113-21.
- Denton, H., Brown, S.M., Roberts, C.W., Alexander, J., McDonald, V., Thong, K.W., and Coombs, G.H. Comparison of the phosphofructokinase and pyruvate kinase activities of *Cryptosporidium parvum*, *Eimeria tenella* and *Toxoplasma gondii*. *Mol. Biochem. Parasitol* 1996; **76**: 23–29.
- Dolejs P, Ditrich O, Machula T, Kalouskova N, Puzova G. Monitoring of *Cryptosporidium* and *Giardia* in Czech drinking water sources. *Schriftenr Ver Wasser Boden Lufthyg* 2000; **105:147-51**.:147-51.
- Donald RG, Roos DS. Insertional mutagenesis and marker rescue in a protozoan parasite: cloning of the uracil phosphoribosyltransferase locus from *Toxoplasma gondii*. *Proc Natl Acad Sci U S A* 1995; **92** (12):5749-53.
- Doyle PS, Crabb J, Petersen C. Anti-*Cryptosporidium parvum* antibodies inhibit infectivity in vitro and in vivo. *Infect Immun* 1993; **61** (10):4079-84.
- DuPont HL, Chappell CL, Sterling CR, *et al.* The infectivity of *Cryptosporidium parvum* in healthy volunteers. *N Engl J Med* 1995; **332** (13):855-9.
- Elliott DA, Clark DP. *Cryptosporidium parvum* induces host cell actin accumulation

- at the host-parasite interface. *Infect Immun* 2000; **68** (4):2315-22.
- Emanuelsson O, von Heijne G. Prediction of organellar targeting signals. *Biochim Biophys Acta* 2001 Dec 12; **1541**(1-2):114-9. Review.
- Embley TM, van der GM, Horner DS, Dyal PL, Foster P. Mitochondria and hydrogenosomes are two forms of the same fundamental organelle. *Philos Trans R Soc Lond B Biol Sci* 2003; **358** (1429):191-201.
- Entrala E, Mascaro C. Glycolytic enzyme activities in *Cryptosporidium parvum* oocysts. *FEMS Microbiol Lett* 1997; **151** (1):51-7.
- Farthing MJ. Clinical aspects of human cryptosporidiosis. *Contrib Microbiol* 2000; **6**:50-74. Review.
- Fayer R. Effect of high temperature on infectivity of *Cryptosporidium parvum* oocysts in water. *Appl Environ Microbiol* 1994; **60** (8):2732-5.
- Fayer R, Morgan U, Upton SJ. Epidemiology of *Cryptosporidium*: transmission, detection and identification. *Int J Parasitol* 2000; **30** (12-13):1305-22.
- Fayer R, Ungar BL. *Cryptosporidium* spp. and cryptosporidiosis. *Microbiol Rev* 1986; **50** (4):458-83.
- Feltus DC, Giddings CW, Schneck BL, *et al.* Evidence supporting zoonotic transmission of *Cryptosporidium* spp. in Wisconsin. *J Clin Microbiol* 2006; **44** (12):4303-8.
- Fritzler JM, Millership JJ, Zhu G. *Cryptosporidium parvum* long-chain fatty acid elongase. *Eukaryot Cell* 2007;**6**(11):2018-28.
- Fujioka M, Takata Y. S-Adenosylhomocysteine hydrolase from rat liver. Purification and some properties. *J Biol Chem* 1981; **256** (4):1631-5.
- Gamra MM, el-Hosseiny LM. Comparative study of the prophylactic and therapeutic effects of paromomycin, recombinant IL-12 alone or in combination against *Cryptosporidium parvum* infection in immunosuppressed mice. *J Egypt Soc Parasitol* 2003; **33** (1):109-22.
- Gardner MJ, Shallom SJ, Carlton JM, *et al.* Sequence of *Plasmodium falciparum*

- chromosomes 2, 10, 11 and 14. *Nature* 2002; **419** (6906):531-4.
- Gatei W, Greensill J, Ashford RW, *et al.* Molecular analysis of the 18S rRNA gene of *Cryptosporidium* parasites from patients with or without human immunodeficiency virus infections living in Kenya, Malawi, Brazil, the United Kingdom, and Vietnam. *J Clin Microbiol* 2003; **41** (4):1458-62.
- Gelius-Dietrich G, Henze K. Pyruvate formate lyase (PFL) and PFL activating enzyme in the chytrid fungus *Neocallimastix frontalis*: a free-radical enzyme system conserved across divergent eukaryotic lineages. *J Eukaryot Microbiol* 2004; **51** (4):456-63.
- Goodman CD, McFadden GI. Fatty acid biosynthesis as a drug target in apicomplexan parasites. *Curr Drug Targets* 2007; **8** (1):15-30.
- Guranowski A, Pawelkiewicz J. Adenosylhomocysteinase from yellow lupin seeds. Purification and properties. *Eur J Biochem* 1977; **80** (2):517-23.
- Guyot K, Follet-Dumoulin A, Lelievre E, *et al.* Molecular characterization of *Cryptosporidium* isolates obtained from humans in France. *J Clin Microbiol* 2001; **39** (10):3472-80.
- Haas CN. Epidemiology, microbiology, and risk assessment of waterborne pathogens including *Cryptosporidium*. *J Food Prot* 2000; **63** (6):827-31.
- Hajdusek O, Ditrich O, Slapeta J. Molecular identification of *Cryptosporidium* spp. in animal and human hosts from the Czech Republic. *Vet Parasitol* 2004; **122** (3):183-92.
- Hansen J, Cherest H, Kielland-Brandt MC. Two divergent MET10 genes, one from *Saccharomyces cerevisiae* and one from *Saccharomyces carlsbergensis*, encode the alpha subunit of sulfite reductase and specify potential binding sites for FAD and NADPH. *J Bacteriol* 1994; **176** (19):6050-8.
- Harris JR, Adrian M, Petry F. Amylopectin: a major component of the residual body in *Cryptosporidium parvum* oocysts. *Parasitology* 2004; **128** (Pt 3):269-82.
- Helland S, Ueland PM. Inactivation of S-adenosylhomocysteine hydrolase by 9-beta-D-arabinofuranosyladenine in intact cells. *Cancer Res* 1982; **42** (3):1130-6.

- Hellard M, Hocking J, Willis J, Dore G, Fairley C. Risk factors leading to *Cryptosporidium* infection in men who have sex with men. *Sex Transm Infect* 2003; **79** (5):412-4.
- Henriquez FL, Richards TA, Roberts F, McLeod R, Roberts CW. The unusual mitochondrial compartment of *Cryptosporidium parvum*. *Trends Parasitol* 2005; **21** (2):68-74.
- Hershfield MS, Aiyar VN, Premakumar R, Small WC. S-Adenosylhomocysteine hydrolase from human placenta. Affinity purification and characterization. *Biochem J* 1985; **230** (1):43-52.
- Hijjawi NS, Meloni BP, Ng'anzo M, *et al.* Complete development of *Cryptosporidium parvum* in host cell-free culture. *Int J Parasitol* 2004; **34** (7):769-77.
- Hoffmeister M, van der KA, Rotte C, *et al.* *Euglena gracilis* rhodoquinone:ubiquinone ratio and mitochondrial proteome differ under aerobic and anaerobic conditions. *J Biol Chem* 2004; **279** (21):22422-9.
- Holy A, Votruba I, Declercq E. Studies on S-Adenosyl-L-Homocysteine Hydrolase .14. Structure-Activity Studies on Open-Chain Analogs of Nucleosides - Inhibition of S-Adenosyl-L-Homocysteine Hydrolase and Antiviral Activity .2. Acid Open-Chain Analogs. *Collection of Czechoslovak Chemical Communications* 1985; **50** (1):262-79.
- Horman A, Korpela H, Sutinen J, Wedel H, Hanninen ML. Meta-analysis in assessment of the prevalence and annual incidence of *Giardia* spp. and *Cryptosporidium* spp. infections in humans in the Nordic countries. *Int J Parasitol* 2004; **34** (12):1337-46.
- Horner DS, Foster PG, Embley TM. Iron hydrogenases and the evolution of anaerobic eukaryotes. *Mol Biol Evol* 2000; **17** (11):1695-709.
- Horner DS, Heil B, Happe T, Embley TM. Iron hydrogenases--ancient enzymes in modern eukaryotes. *Trends Biochem Sci* 2002; **27** (3):148-53.
- Hu Y, Komoto J, Huang Y, *et al.* Crystal structure of S-adenosylhomocysteine hydrolase from rat liver. *Biochemistry* 1999; **38** (26):8323-33.

- Huang BQ, Chen XM, LaRusso NF. *Cryptosporidium parvum* attachment to and internalization by human biliary epithelia in vitro: a morphologic study. *J Parasitol* 2004; **90** (2):212-21.
- Huang J, Mullapudi N, Lancto CA, Scott M, Abrahamsen MS, Kissinger JC. Phylogenomic evidence supports past endosymbiosis, intracellular and horizontal gene transfer in *Cryptosporidium parvum*. *Genome Biol.* 2004; **5** (11): R88.
- Huang Y, Komoto J, Takata Y, *et al.* Inhibition of S-adenosylhomocysteine hydrolase by acyclic sugar adenosine analogue D-eritadenine. Crystal structure of S-adenosylhomocysteine hydrolase complexed with D-eritadenine. *J Biol Chem* 2002; **277** (9):7477-82.
- Insulander M, Lebbad M, Stenstrom TA, Svenungsson B. An outbreak of cryptosporidiosis associated with exposure to swimming pool water. *Scand J Infect Dis* 2005; **37** (5):354-60.
- Inui H, Miyatake K, Nakano Y, Kitaoka S. Occurrence of oxygen-sensitive, NADP+-dependent pyruvate dehydrogenase in mitochondria of *Euglena gracilis*. *J Biochem (Tokyo)* 1984; **96** (3):931-4.
- Inui H, Ono K, Miyatake K, Nakano Y, Kitaoka S. Purification and characterization of pyruvate:NADP+ oxidoreductase in *Euglena gracilis*. *J Biol Chem* 1987; **262** (19):9130-5.
- Inungu JN, Morse AA, Gordon C. Risk factors, seasonality, and trends of cryptosporidiosis among patients infected with human immunodeficiency virus. *Am J Trop Med Hyg* 2000; **62** (3):384-7.
- Jenkins M, Trout JM, Higgins J, *et al.* Comparison of tests for viable and infectious *Cryptosporidium parvum* oocysts. *Parasitol Res* 2003; **89** (1):1-5.
- Jensen JB, Edgar SA. Possible secretory function of the rhoptries of *Eimeria magna* during penetration of cultured cells. *J Parasitol* 1976; **62** (6):988-92.
- Johnson DC, Enriquez CE, Pepper IL, *et al.* Survival of *Giardia*, *Cryptosporidium*, poliovirus and *Salmonella* in marine waters. *Water Science and Technology* 1997; **35** (11-12):261-8.

- Jokipii L, Jokipii AM. Timing of symptoms and oocyst excretion in human cryptosporidiosis. *N Engl J Med* 1986; **315** (26):1643-7.
- Karanis P, Kourenti C, Smith H. Waterborne transmission of protozoan parasites: a worldwide review of outbreaks and lessons learnt. *J Water Health* 2007; **5** (1):1-38.
- Keithly JS, Langreth SG, Buttle KF, Mannella CA. Electron tomographic and ultrastructural analysis of the *Cryptosporidium parvum* relict mitochondrion, its associated membranes, and organelles. *J Eukaryot Microbiol* 2005; **52** (2):132-40.
- Keithly JS, Zhu G, Upton SJ, *et al.* Polyamine biosynthesis in *Cryptosporidium parvum* and its implications for chemotherapy. *Mol Biochem Parasitol* 1997; **88** (1-2):35-42.
- Knudsen RC, Yall I. Partial purification and characterization of S-adenosylhomocysteine hydrolase isolated from *Saccharomyces cerevisiae*. *J Bacteriol* 1972; **112** (1):569-75.
- Korich DG, Mead JR, Madore MS, Sinclair NA, Sterling CR. Effects of ozone, chlorine dioxide, chlorine, and monochloramine on *Cryptosporidium parvum* oocyst viability. *Appl Environ Microbiol* 1990; **56** (5):1423-8.
- Kozisek F, Craun GF, Cerovska L, *et al.* Serological responses to *Cryptosporidium*-specific antigens in Czech populations with different water sources. *Epidemiol Infect* 2007; **135**:1-8.
- Ladda R, Aikawa M, Sprinz H. Penetration of erythrocytes by merozoites of mammalian and avian malarial parasites. *J Parasitol* 1969; **55** (3):633-44.
- LaGier MJ, Tachezy J, Stejskal F, Kutisova K, Keithly JS. Mitochondrial-type iron-sulfur cluster biosynthesis genes (IscS and IscU) in the apicomplexan *Cryptosporidium parvum*. *Microbiology* 2003; **149** (Pt 12):3519-30.
- Leander BS, Harper JT, Keeling PJ. Molecular phylogeny and surface morphology of marine aseptate gregarines (Apicomplexa): *Selenidium* spp. and *Lecudina* spp. *J Parasitol* 2003; **89** (6):1191-205.
- LeChevallier MW, Norton WD, Lee RG. Occurrence of *Giardia* and

- Cryptosporidium* spp. in surface water supplies. *Appl Environ Microbiol* 1991; **57** (9):2610-6.
- Lindmark DG, Muller M. Hydrogenosome, a cytoplasmic organelle of the anaerobic flagellate *Trichomonas foetus*, and its role in pyruvate metabolism. *J Biol Chem* 1973; **248** (22):7724-8.
- Lisle JT, Rose JB. *Cryptosporidium* Contamination of Water in the Usa and Uk - A Minireview. *Journal of Water Supply Research and Technology-Aqua* 1995; **44** (3):103-17.
- Liu C, Vigdorovich V, Kapur V, Abrahamsen MS. A random survey of the *Cryptosporidium parvum* genome. *Infect Immun* 1999; **67** (8):3960-9.
- Lozada-Ramírez JD, Martínez-Martínez I, Sánchez-Ferrer A, García-Carmona F. A colorimetric assay for S-adenosylhomocysteine hydrolase. *J Biochem Biophys Methods*. 2006 Jun 30;**67**(2-3):131-40.
- Lumb R, Smith K, O'Donoghue PJ, Lanser JA. Ultrastructure of the attachment of *Cryptosporidium* sporozoites to tissue culture cells. *Parasitol Res* 1988; **74** (6):531-6.
- MacKenzie WR, Schell WL, Blair KA, *et al.* Massive outbreak of waterborne *Cryptosporidium* infection in Milwaukee, Wisconsin: recurrence of illness and risk of secondary transmission. *Clin Infect Dis* 1995; **21** (1):57-62.
- Madern D, Cai X, Abrahamsen MS, Zhu G. Evolution of *Cryptosporidium parvum* lactate dehydrogenase from malate dehydrogenase by a very recent event of gene duplication. *Mol Biol Evol* 2004; **21** (3):489-97.
- Marshall RJ, Flanigan TP. Paromomycin inhibits *Cryptosporidium* infection of a human enterocyte cell line. *J Infect Dis*. 1992 Apr;**165**(4):772-4.
- Milacek P, Vitovec J. Differential staining of cryptosporidia by aniline-carbol-methyl violet and tartrazine in smears from feces and scrapings of intestinal mucosa. *Folia Parasitol (Praha)* 1985; **32** (1):50.
- Millard PS, Gensheimer KF, Addiss DG, *et al.* An outbreak of cryptosporidiosis from fresh-pressed apple cider. *JAMA* 1994; **272** (20):1592-6.

- Minotto L, Ko GA, Edwards MR, Bagnara AS. *Trichomonas vaginalis*: expression and characterisation of recombinant S-adenosylhomocysteinase. *Exp Parasitol* 1998; **90** (2):175-80.
- Miron D, Kenes J, Dagan R. Calves as a source of an outbreak of cryptosporidiosis among young children in an agricultural closed community. *Pediatr Infect Dis J* 1991; **10** (6):438-41.
- Morpeth SC, Thielman NM. Diarrhea in patients with AIDS. *Curr Treat Options Gastroenterol* 2006; **9** (1):23-37.
- Mudd SH, Poole JR. Labile methyl balances for normal humans on various dietary regimens. *Metabolism* 1975; **24** (6):721-35.
- Muller, M. Energy metabolism. Part I. Anaerobic protozoa. 2003. In: Marr, J. J., Nielsen, T. W. & Komuniecki, R. W. (ed.), *Molecular Medical Parasitology*. Vol. 7. Academic Press, New York. 125–139.
- Muller M. The hydrogenosome. *J Gen Microbiol* 1993; **139** (12):2879-89.
- Nicolet Y, Lemon BJ, Fontecilla-Camps JC, Peters JW. A novel FeS cluster in Fe-only hydrogenases. *Trends Biochem Sci* 2000; **25** (3):138-43.
- Nime FA, Burek JD, Page DL, Holscher MA, Yardley JH. Acute enterocolitis in a human being infected with the protozoan *Cryptosporidium*. *Gastroenterology* 1976; **70** (4):592-8.
- Nixon JE, Field J, McArthur AG, *et al.* Iron-dependent hydrogenases of *Entamoeba histolytica* and *Giardia lamblia*: activity of the recombinant entamoebic enzyme and evidence for lateral gene transfer. *Biol Bull* 2003; **204** (1):1-9.
- Nozaki T, Ali V, Tokoro M. Sulfur-containing amino acid metabolism in parasitic protozoa. *Adv Parasitol* 2005; **60**:1-99.
- O'Handley RM, Cockwill C, McAllister TA, *et al.* Duration of naturally acquired giardiasis and cryptosporidiosis in dairy calves and their association with diarrhea. *J Am Vet Med Assoc* 1999; **214** (3):391-6.
- Okhuysen PC, Chappell CL, Crabb JH, Sterling CR, DuPont HL. Virulence of three distinct *Cryptosporidium parvum* isolates for healthy adults. *J Infect Dis*

1999; **180** (4):1275-81.

Olson ME, Goh J, Phillips M, Guselle N, McAllister TA. *Giardia* cyst and *Cryptosporidium* oocyst survival in water, soil, and cattle feces. Journal of Environmental Quality 1999; **28** (6):1991-6.

Payne SH, Loomis WF. Retention and loss of amino acid biosynthetic pathways based on analysis of whole-genome sequences. Eukaryot Cell 2006; **5** (2):272-6.

Peeters JE, Mazas EA, Masschelein WJ, Villacorta Martiez dM, I, Debacker E. Effect of disinfection of drinking water with ozone or chlorine dioxide on survival of *Cryptosporidium parvum* oocysts. Appl Environ Microbiol 1989; **55** (6):1519-22.

Pegg AE. Polyamine metabolism and its importance in neoplastic growth and a target for chemotherapy. Cancer Res 1988; **48** (4):759-74.

Pereira SJ, Ramirez NE, Xiao L, Ward LA. Pathogenesis of human and bovine *Cryptosporidium parvum* in gnotobiotic pigs. J Infect Dis 2002; **186** (5):715-8.

Pitlik SD, Fainstein V, Garza D, *et al.* Human cryptosporidiosis: spectrum of disease. Report of six cases and review of the literature. Arch Intern Med 1983; **143** (12):2269-75.

Porcelli M, Cacciapuoti G, Fusco S, *et al.* S-adenosylhomocysteine hydrolase from the thermophilic archaeon *Sulfolobus solfataricus*: purification, physico-chemical and immunological properties. Biochim Biophys Acta 1993; **1164** (2):179-88.

Porcelli M, Fusco S, Inizio T, Zappia V, Cacciapuoti G. Expression, purification, and characterization of recombinant S-adenosylhomocysteine hydrolase from the thermophilic archaeon *Sulfolobus solfataricus*. Protein Expr Purif 2000; **18** (1):27-35.

Porcelli M, Moretti MA, Concilio L, *et al.* S-adenosylhomocysteine hydrolase from the archaeon *Pyrococcus furiosus*: biochemical characterization and analysis of protein structure by comparative molecular modeling. Proteins 2005; **58**

(4):815-25.

- Reduker DW, Speer CA, Blixt JA. Ultrastructure of *Cryptosporidium parvum* oocysts and excysting sporozoites as revealed by high resolution scanning electron microscopy. *J Protozool* 1985; **32** (4):708-11.
- Riggs MW, Schaefer DA, Kapil SJ, Barley-Maloney L, Perryman LE. Efficacy of monoclonal antibodies against defined antigens for passive immunotherapy of chronic gastrointestinal cryptosporidiosis. *Antimicrob Agents Chemother* 2002; **46** (2):275-82.
- Riordan CE, Ault JG, Langreth SG, Keithly JS. *Cryptosporidium parvum* Cpn60 targets a relict organelle. *Curr Genet* 2003; **44** (3):138-47.
- Roberts CW, Roberts F, Henriquez FL, *et al.* Evidence for mitochondrial-derived alternative oxidase in the apicomplexan parasite *Cryptosporidium parvum*: a potential anti-microbial agent target. *Int J Parasitol* 2004; **34** (3):297-308.
- Robertson LJ, Campbell AT, Smith HV. Survival of *Cryptosporidium parvum* oocysts under various environmental pressures. *Appl Environ Microbiol* 1992; **58** (11):3494-500.
- Roger AJ, Silberman JD. Cell evolution: mitochondria in hiding. *Nature* 2002; **418** (6900):827-9.
- Rossignol JF. Nitazoxanide in the treatment of acquired immune deficiency syndrome-related cryptosporidiosis: results of the United States compassionate use program in 365 patients. *Aliment Pharmacol Ther* 2006; **24** (5):887-94.
- Rossignol JF, Maisonneuve H. Nitazoxanide in the treatment of *Taenia saginata* and *Hymenolepis nana* infections. *Am J Trop Med Hyg* 1984; **33** (3):511-2.
- Rotte C, Stejskal F, Zhu G, Keithly JS, Martin W. Pyruvate : NADP⁺ oxidoreductase from the mitochondrion of *Euglena gracilis* and from the apicomplexan *Cryptosporidium parvum*: a biochemical relic linking pyruvate metabolism in mitochondriate and amitochondriate protists. *Mol Biol Evol* 2001; **18** (5):710-20.
- Ryan UM, Power M, Xiao L. *Cryptosporidium fayeri* n. sp. (Apicomplexa:

- Cryptosporidiidae) from the Red Kangaroo (*Macropus rufus*). J Eukaryot Microbiol. 2008; **55**(1):22-6.
- Sambrook J and Russell DW. Molecular Cloning: A Laboratory Manual. Cold Spring Harbor Laboratory Press, Cold Spring Harbor, New York. 2001.
- Samie A, Bessong PO, Obi CL, *et al.* *Cryptosporidium* species: preliminary descriptions of the prevalence and genotype distribution among school children and hospital patients in the Venda region, Limpopo Province, South Africa. Exp Parasitol 2006; **114** (4):314-22.
- Schanche JS, Schanche T, Ueland PM, Holy A, Votruba I. The effect of aliphatic adenine analogues on S-adenosylhomocysteine and S-adenosylhomocysteine hydrolase in intact rat hepatocytes. Mol Pharmacol 1984; **26** (3):553-8.
- Schrével J. Observations biologique et ultrastructurales sur les Selenidiidae et leurs conséquences sur la systematique des gregarinomorphes. J Protozool 1971; **18**, 448–470.
- Sebestova L, Votruba I, Holy A. Studies on S-Adenyl-L-Homocysteine Hydrolase .11. S-Adenosine-L-Homocysteine Hydrolase from Nicotiana-Tabacum-l - Isolation and Properties. Collection of Czechoslovak Chemical Communications 1984; **49** (6):1543-51.
- Shimizu S, Shiozaki S, Ohshiro T, Yamada H. Occurrence of S-adenosylhomocysteine hydrolase in prokaryote cells. Characterization of the enzyme from *Alcaligenes faecalis* and role of the enzyme in the activated methyl cycle. Eur J Biochem 1984; **141** (2):385-92.
- Sibley LD. Intracellular parasite invasion strategies. Science 2004; **304** (5668):248-53.
- Slapeta J. Web page: iCRYPTO – Taxonomy of *Cryptosporidium*. <http://www.vetsci.usyd.edu.au/staff/JanSlapeta/> 2007.
- Slapeta J, Keithly JS. *Cryptosporidium parvum* mitochondrial-type HSP70 targets homologous and heterologous mitochondria. Eukaryot Cell 2004; **3** (2):483-94.
- Slapeta J, Stejskal F, Keithly JS. Characterization of S-adenosylmethionine

- synthetase in *Cryptosporidium parvum* (Apicomplexa). FEMS Microbiol Lett 2003; **225** (2):271-7.
- Slavin D. *Cryptosporidium meleagridis* (sp. nov.). J Comp Pathol 1955; **65** (3):262-6.
- Smith NH, Cron S, Valdez LM, Chappell CL, White AC, Jr. Combination drug therapy for cryptosporidiosis in AIDS. J Infect Dis 1998; **178** (3):900-3.
- Staunton J, Weissman KJ. Polyketide biosynthesis: a millennium review. Nat Prod Rep 2001; **18** (4):380-416.
- Stejskal F, Slapeta J, Ctrnacta V, Keithly JS. A Narf-like gene from *Cryptosporidium parvum* resembles homologues observed in aerobic protists and higher eukaryotes. FEMS Microbiol Lett 2003; **229** (1):91-6.
- Striepen B, Pruijssers AJ, Huang J, *et al.* Gene transfer in the evolution of parasite nucleotide biosynthesis. Proc Natl Acad Sci U S A 2004; **101** (9):3154-9.
- Strong WB, Nelson RG. Preliminary profile of the *Cryptosporidium parvum* genome: an expressed sequence tag and genome survey sequence analysis. Mol Biochem Parasitol. 2000 Mar 15;**107**(1):1-32.
- Tamburrini A, Pozio E. Long-term survival of *Cryptosporidium parvum* oocysts in seawater and in experimentally infected mussels (*Mytilus galloprovincialis*). Int J Parasitol 1999; **29** (5):711-5.
- Tanaka N, Nakanishi M, Kusakabe Y, *et al.* Crystal structure of S-adenosyl-L-homocysteine hydrolase from the human malaria parasite *Plasmodium falciparum*. J Mol Biol 2004; **343** (4):1007-17.
- Tangermann RH, Gordon S, Wiesner P, Kreckman L. An outbreak of cryptosporidiosis in a day-care center in Georgia. Am J Epidemiol 1991; **133** (5):471-6.
- Tetley L, Brown SM, McDonald V, Coombs GH. Ultrastructural analysis of the sporozoite of *Cryptosporidium parvum*. Microbiology 1998; **144** (Pt 12):3249-55.
- Thompson RC, Olson ME, Zhu G, *et al.* *Cryptosporidium* and cryptosporidiosis. Adv

- Parasitol 2005; **59:77-158**.:77-158.
- Tovar J, Fischer A, Clark CG. The mitosome, a novel organelle related to mitochondria in the amitochondrial parasite *Entamoeba histolytica*. Mol Microbiol 1999; **32** (5):1013-21.
- Tovar J, Leon-Avila G, Sanchez LB, *et al.* Mitochondrial remnant organelles of *Giardia* function in iron-sulphur protein maturation. Nature 2003; **426** (6963):172-6.
- Tumwine JK, Kekitiinwa A, Bakeera-Kitaka S, *et al.* Cryptosporidiosis and microsporidiosis in ugandan children with persistent diarrhea with and without concurrent infection with the human immunodeficiency virus. Am J Trop Med Hyg 2005; **73** (5):921-5.
- Turner MA, Yang X, Yin D, *et al.* Structure and function of S-adenosylhomocysteine hydrolase. Cell Biochem Biophys 2000; **33** (2):101-25.
- Tyzzar EE. A sporozoan found in the peptic glands of the common mouse. Proc Soc Exp Biol Med 1907; **5**:12-13.
- Tyzzar EE. *Cryptosporidium parvum* (sp. nov.), a coccidium found in the small intestine of the common mouse. Arch Protistenkd 1912; **26**:394–412.
- Umejiego NN, Li C, Riera T, Hedstrom L, Striepen B. *Cryptosporidium parvum* IMP dehydrogenase: identification of functional, structural, and dynamic properties that can be exploited for drug design. J Biol Chem 2004; **279** (39):40320-7.
- Umejiego NN, Gollapalli D, Sharling L, Volftsun A, Lu J, Benjamin NN, Stroupe AH, Riera TV, Striepen B, Hedstrom L. Targeting a Prokaryotic Protein in a Eukaryotic Pathogen: Identification of Lead Compounds against Cryptosporidiosis. Chem Biol 2008;**15**(1):70-7
- Upton SJ, Tilley M, Brillhart DB. Effects of select medium supplements on in vitro development of *Cryptosporidium parvum* in HCT-8 cells. J Clin Microbiol. 1995 Feb;**33**(2):371-5.
- Wheeler C, Vugia DJ, Thomas G, *et al.* Outbreak of cryptosporidiosis at a California waterpark: employee and patron roles and the long road towards prevention.

- Epidemiol Infect 2007; **135** (2):302-10.
- Williams BA, Hirt RP, Lucocq JM, Embley TM. A mitochondrial remnant in the microsporidian *Trachipleistophora hominis*. Nature 2002; **418** (6900):865-9.
- Williams BA, Keeling PJ. Cryptic organelles in parasitic protists and fungi. Adv Parasitol. 2003; **54**:9-68. Review.
- Winzeler EA, Shoemaker DD, Astromoff A, *et al.* Functional characterization of the *S. cerevisiae* genome by gene deletion and parallel analysis. Science 1999; **285** (5429):901-6.
- Wongstitwilairoong B, Srijan A, Serichantalergs O, *et al.* Intestinal parasitic infections among pre-school children in Sangkhlaburi, Thailand. Am J Trop Med Hyg 2007; **76** (2):345-50.
- Xiao L, Bern C, Limor J, *et al.* Identification of 5 types of *Cryptosporidium* parasites in children in Lima, Peru. J Infect Dis 2001; **183** (3):492-7.
- Xu P, Widmer G, Wang Y, *et al.* The genome of *Cryptosporidium hominis*. Nature 2004; **431** (7012):1107-12.
- Yang X, Hu Y, Yin DH, *et al.* Catalytic strategy of S-adenosyl-L-homocysteine hydrolase: transition-state stabilization and the avoidance of abortive reactions. Biochemistry 2003; **42** (7):1900-9.
- Yarlett N. Polyamine biosynthesis and inhibition in *Trichomonas vaginalis*. Parasitol Today 1988; **4** (12):357-60.
- Yuan CS, ult-Riche DB, Borchardt RT. Chemical modification and site-directed mutagenesis of cysteine residues in human placental S-adenosylhomocysteine hydrolase. J Biol Chem 1996; **271** (45):28009-16.
- Yuan CS, Yeh J, Liu S, Borchardt RT. Mechanism of inactivation of S-adenosylhomocysteine hydrolase by (Z)-4',5'-didehydro-5'-deoxy-5'-fluoroadenosine. J Biol Chem 1993; **268** (23):17030-7.
- Zhu G. Current progress in the fatty acid metabolism in *Cryptosporidium parvum*. J Eukaryot Microbiol 2004; **51** (4):381-8.

- Zhu G, Keithly JS. Alpha-proteobacterial relationship of apicomplexan lactate and malate dehydrogenases. *J Eukaryot Microbiol* 2002; **49** (3):255-61.
- Zhu G, Keithly JS. Molecular analysis of a P-type ATPase from *Cryptosporidium parvum*. *Mol Biochem Parasitol*. 1997 Dec 1; **90**(1):307-16.
- Zhu G, Keithly JS, Philippe H. What is the phylogenetic position of *Cryptosporidium*? *Int J Syst Evol Microbiol* 2000; **50 Pt 4:1673-81**.:1673-81.
- Zhu G, LaGier MJ, Stejskal F, *et al.* *Cryptosporidium parvum*: the first protist known to encode a putative polyketide synthase. *Gene* 2002; **298** (1):79-89.
- Zhu G, Li Y, Cai X, *et al.* Expression and functional characterization of a giant Type I fatty acid synthase (*CpFASI*) gene from *Cryptosporidium parvum*. *Mol Biochem Parasitol* 2004; **134** (1):127-35.
- Zimmerman TP, Wolberg G, Duncan GS, Elion GB. Adenosine analogues as substrates and inhibitors of S-adenosylhomocysteine hydrolase in intact lymphocytes. *Biochemistry* 1980; **19** (10):2252-9.

APENDIX A**ARTICLE 1****LOCALIZATION OF PYRUVATE:NADP⁺ OXIDOREDUCTASE IN
SPOROZOITES OF *Cryptosporidium parvum***

Vlasta Čtrnáctá,^a Jeffrey G. Ault,^b František Stejskal,^a and Janet S. Keithly,^{b,c}

^aDepartment of Tropical Medicine, 1st Faculty of Medicine, Charles University in Prague, Prague, Czech Republic

^bNew York State Department of Health, Wadsworth Center, Albany, New York, USA

^cDepartment of Biomedical Sciences, School of Public Health, State University of New York, Albany, New York, USA

Published in J Eukaryot Microbiol 2006; **53**(4): 225–231.

APENDIX B**ARTICLE 2****A *NARF*-LIKE GENE FROM *Cryptosporidium parvum* RESEMBLES
HOMOLOGUES OBSERVED IN ANEROBIC PROTISTS AND HIGHER
EUKARYOTES**

František Stejskal,^a Jan Šlapeta,^b Vlasta Čtrnáctá,^a and Janet S. Keithly,^b

^aDepartment of Tropical Medicine, 1st Faculty of Medicine, Charles University in Prague, Prague, Czech Republic

^bNew York State Department of Health, Wadsworth Center, Albany, New York, USA

Published in FEMS Microbiol Lett 2003; **229**: 91–96.

APENDIX C**ARTICLE 3****CHARACTERIZATION OF S-ADENOSYLHOMOCYSTEINE HYDROLASE
FROM *Cryptosporidium parvum***

Vlasta Čtrnáctá,^a František Stejskal,^a Janet S. Keithly,^b and Ivan Hrdý,^c

^aDepartment of Tropical Medicine, 1st Faculty of Medicine, Charles University in Prague, Prague, Czech Republic

^bNew York State Department of Health, Wadsworth Center, Albany, New York, USA

^cDepartment of Parasitology, Faculty of Science, Charles University in Prague, Prague, Czech Republic

Published in FEMS Microbiol Lett 2007; **273**: 87–95.

CURRICULUM VITAE

- Name: Vlasta Čtrnáctá
- Nationality: Czech
- Address: Pod strojírnami 708/4, 190 02 Praha, Czech Republic
- Email Address: ctrnacta@yahoo.com
-
- Education: B.A., Biology, Science Faculty, the Charles University in Prague, Czech Republic, 1996
M.S., Immunology, Science Faculty, the Charles University in Prague, Czech Republic, 1998
-
- Current position: Research Associate, Department of Gene Expression, BTU Academy of Sciences, Czech Republic, 2008 - present
- Research Associate and PhD. student at the Department of Tropical Diseases, 1st Faculty of Medicine, the Charles University in Prague, Czech Republic, 2002 - present
-
- Research experience:
- Research Associate, Department of Cell Biology, 1st Faculty of Medicine, Prague, Czech Republic, 1998 – 2000
- ERASMUS/SOCRATES Fellow, Department of Cytology and Genetics, University of Vienna, Vienna, Austria, March - May 2000
- Research Associate, Department of Cardiovascular Sciences, Albany Medical College, Albany, NY, USA, 2000 – 2002
- Fogarty Fellow, Department of Parasitology, Wadsworth Center, NYS DOH, Albany, NY, USA, February - August 2004
- Fogarty Fellow, Department of Parasitology, Wadsworth Center, NYS DOH, Albany, NY, USA, July - August 2005
- Fogarty Fellow, Department of Veterinary Pathobiology, Texas A&M University, College Station, TX, USA, November – February 2007 - 2008
-
- Languages: English, Russian, Spanish

Grants: Principal Investigator

S-adenosylhomocystein Hydrolase from the Parasitic Protist *Cryptosporidium parvum*: Characterization of the Recombinant Protein and its Inhibitors. The Grant of the Grant Agency of Charles University 29/05. 2005-2006

Collaborator

Characterization and in vitro expression of the *Cryptosporidium parvum* iron-hydrogenase (HDG) gene. Reentry grant: National Institute of Health - Fogarty International Center (NIH-FIC), Bethesda, USA, 5D43TW0091504. 2002-2003

Dangerous and newly expanding infections. The Fond of Development for Universitites, Czech Republic, 982. 2004

Molecular Biology and Pathology of the Cell. The Grant of Ministry of Education, Czech Republic, MSM 0021620806. 2005-present

Inovations of the Tropical Medicine and the Medical Parasitology Lectures at the First Faculty of Medicine, Charles University in Prague. The Fond of Development for Universitites, Czech Republic, 1694. 2006

Grant Agency of the Academy of Sciences of the Czech Republic, IAA500520809. 2008 – 2010. Mechanisms of embryonic stem cells early differentiation.

List of publications:

Koberna K, Stanek D, Malinsky J, Eltsov J, Pliss A, **Ctrnacta V**, Cermanova S, Raska I. Nuclear Organization Studied with the Help of a Hypotonic Shift: Its Use Permits Hydrophilic Molecules to Enter into Living Cells. *Chromosoma* 1999. Sep, **108**(5): 325-35

Koberna K, Stanek D, Malinsky J, **Ctrnacta V**, Cermanova S, Novotna J, Kopsky J, Raska I. *In situ* Fluorescence Visualization of Bromouridine Incorporated into Newly Transcribed Nucleolar RNA. *Acta Histochem* 2000; Feb, **102**(1):15-20

Zou Z, DiRusso CC, **Ctrnacta V**, Black PN. Fatty Acid Transport in *Saccharomyces cerevisiae*. Directed Mutagenesis of FAT1 Distinguishes the Biochemical Activities Associated with FAT1p. *J Biol Chem* 2002; Aug 23, **277**(34): 31062-71

- Stejskal F, Slapeta J, **Ctrnacta V**, Keithly JS. A Narf-like gene from *Cryptosporidium parvum* resembles homologues observed in aerobic protists and higher eukaryotes. FEMS Microbiol Lett 2003; **229** (1): 91-6
- Tong F, Black PN, Bivins L, Quackenbush S, **Ctrnacta V**, Dirusso CC. Direct interaction of *Saccharomyces cerevisiae* Faa1p with the Omi/HtrA protease orthologue Ynm3p alters lipid homeostasis. Mol Genet Genomics 2006; Feb **10**: 1-14
- Ctrnacta V**, Ault JG, Stejskal F, Keithly JS. Localization of pyruvate:NADP⁺ oxidoreductase in sporozoites of *Cryptosporidium parvum*. J Eukaryot Microbiol 2006; **53** (4):225-31
- Ctrnacta V**, Stejskal F, Keithly JS, Hrdy I. Characterization of S-adenosylhomocysteine hydrolase from *Cryptosporidium parvum*. FEMS Microbiol Lett 2007; **273** (1):87-95